

THE SOLUTION OF STEADY-STATE FREE SURFACE PROBLEMS

BY THE FINITE ELEMENT METHOD

L H G S CHANDRASIRI

University of Cape Town

The copyright of this thesis vests in the author. No quotation from it or information derived from it is to be published without full acknowledgement of the source. The thesis is to be used for private study or non-commercial research purposes only.

Published by the University of Cape Town (UCT) in terms of the non-exclusive license granted to UCT by the author.

**THE SOLUTION OF STEADY-STATE FREE SURFACE PROBLEMS
BY THE FINITE ELEMENT METHOD**

by

L H G S CHANDRASIRI
B.Sc. (Hons)

A thesis submitted to the
UNIVERSITY OF CAPE TOWN
in fulfilment of the requirements for the degree of
MASTER OF SCIENCE

Department of Applied Mathematics
University of Cape Town

March 1992

The University of Cape Town has been given
the right to reproduce this thesis in whole
or in part. Copyright is held by the author.

DECLARATION OF CANDIDATE

I hereby declare that this thesis is my own work and that it has not been submitted for a degree at any other university.

Signed by candidate

Signature Removed

L H G S CHANDRASIRI

To my children,
Wathsala, Shashikala and Ravi

TABLE OF CONTENTS

ACKNOWLEDGEMENTS		i
ABSTRACT		ii
CHAPTER 1	INTRODUCTION	1
CHAPTER 2	STEADY-STATE FREE SURFACE PROBLEM FOR VISCOUS FLOWS	8
2.1	Basic Flow Equations	8
2.2	Boundary Conditions	10
2.3	Dimensionless Form of Equations	12
2.4	Variational or Weak Formulation	14
2.5	The Normal Stress Equation	18
CHAPTER 3	FINITE ELEMENT APPROXIMATIONS	21
3.1	The Auxiliary Problem	21
3.2	Finite Element Approximations	24
3.3	Calculation of Element Matrices	32
3.4	Numerical Integration	38
3.5	The Normal Stress Equation	39
3.6	Stress Extrapolation	42
3.7	Discrete Form of the Normal Stress Equation	45
CHAPTER 4	SOLUTION ALGORITHM AND NUMERICAL RESULTS	48
4.1	Solution Algorithm	48
4.2	Numerical Results	52
CHAPTER 5	DISCUSSION AND CONCLUSIONS	62
REFERENCES		64

ACKNOWLEDGEMENTS

I would like to express my deep gratitude to the supervisor of this thesis, Professor B D Reddy, for his patience, guidance and support during the study.

I would also like to thank Mr Robin Eve for his valuable assistance throughout this study.

Many thanks and appreciation to my wife Latha, for all her help, encouragement and patience during her stay with our children in Cape Town.

It is my pleasure to thank Mrs Shirley Breed for typing this document.

Finally, I would like to thank the Foundation for Research Development and the FRD/UCT Centre for Research in Computational and Applied Mechanics for making it financially possible for me to complete a Master's degree.

ABSTRACT

This thesis is concerned with the development of a variational formulation for the problem of viscous incompressible free surface flows, and with the development and implementation of algorithms for the solution of this problem by finite elements. The study is restricted to two-dimensional steady problems.

The approach differs from those in current use, in that it is based on a two-stage strategy suggested by theoretical (existence) studies of the problem. In the first stage the free surface is kept fixed and the resulting so-called auxiliary problem is solved. In the second stage the equation for the normal stress on the free surface is used to update the free surface. Both the auxiliary problem and the normal stress equation are formulated variationally; in the case of the latter problem the unknown variable is actually the slope of the free surface. Finite element approximations are used in both problems.

Algorithms are developed for determining solutions at the two stages, and for the overall problem. The key example treated is the die-swell problem, for the plane and axisymmetric cases. Solutions obtained by the present method are presented, and compared with the solutions of others where available.

CHAPTER 1

INTRODUCTION

A fluid is a substance (gas or liquid) that will deform continuously under the action of applied surface (shearing) stresses.

Different fluids show different relations between stress and the rate of deformation. Depending on the nature of relation followed between stress and rate of deformation, a fluid can be classified as Newtonian or non-Newtonian. A Newtonian fluid is one in which the shear stress is directly proportional to the rate of deformation. The constant of proportionality is defined as μ , the absolute or dynamic viscosity. Common examples of Newtonian fluids are air and water. A non-Newtonian fluid is one which has a variable proportionality between stress and rate of deformation. Common examples of non-Newtonian fluids are some of the plastics, colloidal suspensions and emulsions.

Fluids can also be divided into two categories depending on the property of compressibility. Usually fluids are treated as incompressible while gases and vapours are assumed to be compressible.

A flow may be termed as inviscid or viscous depending on the importance of consideration of viscosity of the fluid in the analysis. An inviscid flow is a frictionless flow characterized by zero

viscosity. A viscous flow is one in which the fluid is assumed to have non-zero viscosity. Although no real fluid is inviscid, there are several flow situations in which the effect of viscosity of the fluid can be neglected. For example, in the analysis of a flow over a body surface, the viscosity effects are considered in a thin region close to the flow boundary (known as the boundary layer) while the viscosity effect is neglected in the rest of the flow.

The equations which describe the motion of viscous incompressible fluids are the Navier-Stokes equations. These are due to Navier in 1827 and, independently, Stokes in 1847. While the behaviour of many fluids is satisfactorily described by these equations, they are difficult to solve in realistic cases, so that approximate solution methods are of great importance.

Free surface flows

A free surface flow is a problem of fluid flow in which part of the boundary, identified as the free surface of the fluid, is unknown. Free boundaries occur in a wide variety of physical phenomena including jets, flows over weirs, ground water flows under dam walls, ice melting in water, sluice gate flows, and the coating of materials with thin films (see, for example, Ruschak and Scriven (1977)).

Free surface flows are particularly difficult, if not impossible, to solve in closed form so that many numerical schemes have been devised for this purpose. We are particularly interested in finite element

approximations of these problems, and some of the relevant work is now reviewed. Some comments on finite-difference approaches are also made.

Nickell, Tanner and Caswell (1974) used a stream-surface scheme to solve by the finite element method the problem of the creeping Newtonian jet. Tanner, Nickell and Bilger (1975) extended the computation to non-Newtonian liquids. Stream-surface schemes and the finite element method have also been used by Thompson, Mark and Lin (1969) for slow flow of an incompressible non-Newtonian liquid and by Chan and Larock (1973) and Larock and Taylor (1976) for a potential jet. All of these investigators neglected capillary pressure, that is, the effect of surface tension was excluded.

Williamson (1972) included the effect of surface tension and employed successfully a normal-stress scheme. He studied the flow where two flexible but inextensible strips with viscous liquid between them are pulled apart as they emerge from passing between a pair of cylindrical rollers. He neglected inertial effects and solved the resulting biharmonic equation for the stream function by means of a finite-difference rather than finite element method. Williamson represented the entire free surface of interest by a single sixth-degree polynomial with two adjustable parameters. These were adjusted in each iteration to minimize the residual in the normal-stress boundary conditions.

Jean and Pritchard (1980) reported on experimental observations relating to the solution of certain free surface flows when a fluid is extruded from a nozzle. They described how the free surface does not necessarily separate from the nozzle at a sharp edge, and furthermore illustrated some of the differences between the flow of a Newtonian fluid and that of a non-Newtonian fluid. They also discussed the die-swell phenomenon which has many practical applications, the best known of which are the extrusion of materials from dies and the coating of surfaces with emulsions.

Boundary-fitted coordinate techniques have been successfully applied to free surface flow problems by Haussling and Coleman (1979), and by Chan and Chan (1980).

Omodei (1979) investigated the behaviour and shape of the free surface for the die-swell problem, with special emphasis on the "die-swell" ratio. In his numerical results, obtained by the finite element method, he reports on the shape of the free surface and the "die-swell" ratio for a range of values of the significant parameters. He solved the die-swell problem for values of the Reynolds number ranging from 0.001 to 1000, and for various choices of the surface tension parameter. Omodei (1980) extended the results in the 1979 work to the case of axisymmetric problems, using the same procedures as in the earlier paper.

Asaithambi (1987) introduced a finite difference method for an accurate and efficient solution of potential flows with a free

surface. He used boundary fitted coordinates, which allow the problem to be solved in a mapped domain composed solely of rectangles, which overcome the difficulties introduced by the free surface.

Kruyt, Cuvelier, Segal and van der Zanden (1988) introduced a total linearization method for solving steady viscous free boundary flow problems (including capillary effects) by the finite element method. Numerical experiments show that the iterative method gives accurate results and converges very fast.

Cuvelier and Schulkes (1990) presented a comprehensive survey of numerical methods for viscous free surface problems, both steady and unsteady. They discussed static free boundary problems governed by the Laplace-Young equation in two- and three-dimensional containers. They also formulated and solved numerically two-dimensional stationary free boundary problems governed by the Navier-Stokes equations, and a thermocapillary free boundary problem governed by the Navier-Stokes equations coupled with the heat equation.

Ho and Patera (1990) described a new Legendre spectral method for the solution of unsteady incompressible viscous free surface flows. They presented a new variational formulation using an Arbitrary-Lagrangian Eulerian (ALE) description in which the mesh points deform independently of the fluid particles. They presented detailed results for the spectral element simulation of the film flow problem. In a more recent paper Ho and Patera (to appear) investigated three-dimensional viscous free surface flows with natural imposition of

surface tension boundary conditions. They illustrated this by a finite (spectral) element unsteady Navier-Stokes analysis of the stability of a falling liquid film. This problem is equivalent in structure to the die-swell problem.

Georgios, Schultz and Olson (1990) use the singular Finite Element Method to solve the sudden-expansion and the die-swell problem, in order to improve the accuracy of the solution in the vicinity of the singularity and to speed up the convergence. Results were obtained for various Reynolds numbers up to 100, using the singular elements constructed for the creeping flow problem. The die-swell problem is solved using the singular elements constructed for the stick-slip condition.

The present study

The aim of this study is to introduce and implement a new finite element method for analysis of steady viscous free surface flows. The study is confined to plane and axisymmetric problems. The basis for the solution method is a predictor-corrector strategy used in theoretical analyses of this problem, for example by Pukhnachov (1972) and by le Roux and Reddy (1991).

The strategy is as follows:

1. Predictor step

The free surface is fixed and the steady Navier-Stokes problem is solved for the velocity u and pressure p .

2. Corrector step

The equation for the normal stress on the free surface is solved, using u and p from the predictor step, for the new free surface. This procedure is carried out iteratively until convergence is achieved, to within an acceptable tolerance.

A novel feature of the method is that in the corrector step, the equation for the free surface is formulated variationally and also solved by finite elements.

The plan of the remainder of the thesis is as follows: in Chapter 2 the equations of the problem are introduced, and the variational problem is formulated. Chapter 3 is concerned with the details of the finite element approximations. Finally, in Chapter 4 the algorithms for solution of the free surface problem are discussed, and applied to the die-swell problem. Both the plane and axisymmetric problems are considered, and results are compared with existing results, where they exist. We conclude with a short discussion in Chapter 5.

CHAPTER 2

STEADY-STATE FREE SURFACE PROBLEM FOR VISCOUS FLOWS

2.1 BASIC FLOW EQUATIONS

We consider the motion in a domain $\Omega \subset \mathbb{R}^2$ of a fluid which is isothermal, incompressible and Newtonian with constant density ρ and viscosity μ . With these assumptions the equations of steady flow, which are the equations of conservation of momentum and of mass, reduce to the *Navier-Stokes* equations

$$\left. \begin{aligned} \operatorname{div} \mathbf{T} + \rho \mathbf{f} &= \rho (\nabla \mathbf{u}) \mathbf{u} \\ \operatorname{div} \mathbf{u} &= 0 \end{aligned} \right\} \text{ on } \Omega \quad . \quad \begin{array}{l} (2.1) \\ (2.2) \end{array}$$

Here $\mathbf{T} = -p\mathbf{I} + 2\mu \mathbf{D}(\mathbf{u})$ is the stress, $\mathbf{D}(\mathbf{u}) = \frac{1}{2} (\nabla \mathbf{u} + (\nabla \mathbf{u})^T)$ is the deformation rate tensor, and \mathbf{f} is the body force; \mathbf{u} denotes the velocity vector and p the pressure.

The components of \mathbf{D} are given by

$$[\mathbf{D}] = \begin{bmatrix} \frac{\partial u_1}{\partial x_1} & \frac{1}{2} \left[\frac{\partial u_1}{\partial x_2} + \frac{\partial u_2}{\partial x_1} \right] & 0 \\ \frac{1}{2} \left[\frac{\partial u_1}{\partial x_2} + \frac{\partial u_2}{\partial x_1} \right] & \frac{\partial u_2}{\partial x_2} & 0 \\ 0 & 0 & a \frac{u_2}{x_2} \end{bmatrix}$$

for the case in which $\mathbf{u} = \mathbf{u}(x_1, x_2)$; here and henceforth the constant a is defined by

$$a = \begin{cases} 0 & \text{for plane problems with } (x_1, x_2) = (x, y) \\ & \text{(Cartesian coordinates)} \\ 1 & \text{for axisymmetric problems with} \\ & (x_1, x_2) = (z, r) \text{ (polar coordinates)} \end{cases} .$$

Substituting for \mathbf{T} in (2.1) the Navier-Stokes equations become

$$-\nabla p + 2\mu \operatorname{div} \mathbf{D}(\mathbf{u}) + \rho(\nabla \mathbf{u})\mathbf{u} = \rho \mathbf{f}$$

or, using (2.2),

$$\left. \begin{aligned} -\mu\nabla^2\mathbf{u} + \nabla p + \rho(\nabla\mathbf{u})\mathbf{u} &= \rho\mathbf{f} \\ \text{div } \mathbf{u} &= 0 \end{aligned} \right\} \text{ in } \Omega \quad (2.3)$$

$$\left. \begin{aligned} -\mu\nabla^2\mathbf{u} + \nabla p + \rho(\nabla\mathbf{u})\mathbf{u} &= \rho\mathbf{f} \\ \text{div } \mathbf{u} &= 0 \end{aligned} \right\} \text{ in } \Omega \quad (2.4)$$

2.2 BOUNDARY CONDITIONS

The flow is subject to various boundary conditions in general, which we now describe. Suppose the domain Ω has boundary Γ : this may be subdivided into non-overlapping subsets Γ_i , Γ_o , Γ_s , Γ_w and Γ_f , with boundary conditions

$$\mathbf{u} = \mathbf{u}_i \quad \text{on } \Gamma_i \text{ (inlet velocity),} \quad (2.5a)$$

$$\mathbf{u} = \mathbf{u}_o \quad \text{on } \Gamma_o \text{ (outlet velocity),} \quad (2.5b)$$

$$\mathbf{u} = \mathbf{0} \quad \text{on } \Gamma_w \text{ (non-slip condition),} \quad (2.5c)$$

$$\left. \begin{aligned} u_n &= 0 \\ \mathbf{Tn} \cdot \mathbf{t} &= 0 \end{aligned} \right\} \text{ on } \Gamma_s \text{ (symmetry condition),} \quad (2.5d)$$

$$\left. \begin{aligned} u_n &= 0 \\ \mathbf{Tn} \cdot \mathbf{t} &= 0 \end{aligned} \right\} \text{ on } \Gamma_f \text{ (free surface condition),} \quad (2.5e)$$

$$\mathbf{Tn} \cdot \mathbf{n} = \sigma K \quad \text{on } \Gamma_f \text{ (free surface condition),} \quad (2.5f)$$

where \mathbf{n} and \mathbf{t} denote the unit normal and tangent to the boundary, and $u_n = \mathbf{u} \cdot \mathbf{n}$ is the normal component of velocity. These conditions are illustrated in Figure 2.1 for the case of the die-swell problem.

The boundary condition (2.5d) holds on that part of the boundary which is an axis of symmetry, and describes the fact that the normal velocity u_n is zero, while the tangential component $Tn \cdot t$ of surface traction is zero. The free surface conditions (2.5e) and (2.5f) express the fact that the normal velocity is zero, while the normal component of surface traction is proportional to the curvature K of the surface, the constant of proportionality being the surface tension coefficient σ .

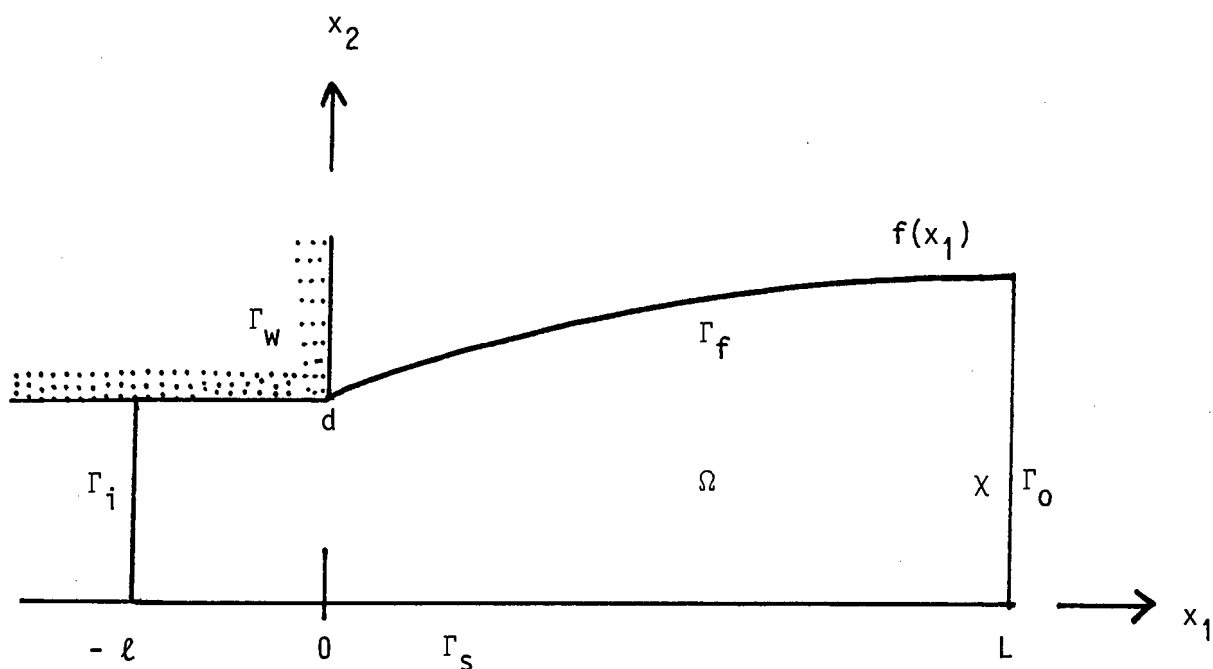


Figure 2.1 : Illustration of boundary conditions for the case of the die-swell problem

Note that there is one more equation on Γ_f than is required. This extra equation will allow us to solve for the free surface Γ_f , whose shape is not known *a priori*.

We will be interested in *plane* and *axisymmetric* problems. In both these cases the free surface is defined by a function $x_2 = f(x_1)$ where $(x_1, x_2) = (x, y)$ (Cartesian coordinates) for a plane problem, and $(x_1, x_2) = (z, r)$ (cylindrical polar coordinates) for an axisymmetric problem. In these cases the curvature is given in terms of f by (Dym (1974), p.15, Joseph (1976))

$$K(f) = \left[\frac{f'}{\sqrt{1 + (f')^2}} \right]' + a \left[\frac{1}{f \sqrt{1 + (f')^2}} \right] . \quad (2.6)$$

2.3 DIMENSIONLESS FORM OF EQUATIONS

We begin by deriving a non-dimensional form of the Navier-Stokes equations. Let d be a characteristic length and U a characteristic velocity. Define dimensionless variables by

$$\bar{\mathbf{x}} = \frac{\mathbf{x}}{d} , \quad \bar{\mathbf{u}}(\bar{\mathbf{x}}) = \frac{\mathbf{u}(\mathbf{x})}{U} , \quad \bar{p}(\bar{\mathbf{x}}) = \frac{p(\mathbf{x})}{\rho U^2} , \quad \bar{f}(\bar{\mathbf{x}}) = \frac{f(\mathbf{x})d}{U^2} .$$

We also introduce the Reynolds number $Re = dU\rho/\mu$. With this change of variables the Navier-Stokes equations become

$$(\nabla \bar{\mathbf{u}}) \bar{\mathbf{u}} - \text{div } \bar{\mathbf{T}} = \bar{\mathbf{f}} , \quad (2.7)$$

$$\text{div } \bar{\mathbf{u}} = 0 , \quad (2.8)$$

where $\bar{T}(\bar{u}, \bar{p}) = -\bar{p}\mathbf{I} + \frac{2}{\text{Re}} \bar{D}(\bar{u})$, $\bar{D}(\bar{u}) = \frac{1}{2}(\nabla\bar{u} + \nabla^T\bar{u})$ and the divergences and gradients are with respect to \bar{x} .

The boundary conditions (2.5) may also be recast in non-dimensional form. Equations (2.5a-e) are dealt with simply by replacing u by \bar{u} (and u_i by $\bar{u}_i = u_i/U$ in (2.7a)) and T by \bar{T} . To obtain the non-dimensional form of (2.5f) we first set

$\bar{f}(\bar{x}_1) = f(x_1)/d$. Then (2.5f) becomes

$$\frac{(\text{Re})^2}{S} \bar{T}\mathbf{n} \cdot \mathbf{n} = \bar{K}(\bar{f}) \quad (2.9)$$

where $S = \rho\sigma d/\mu^2$, $\bar{f}(\bar{x}_1) = f(x_1)/d$ and

$$\bar{K}(\bar{f}) = \left[\frac{\bar{f}'}{\sqrt{1 + (\bar{f}')^2}} \right]' + a \left[\frac{1}{\bar{f}\sqrt{1 + (\bar{f}')^2}} \right],$$

the derivatives here being with respect to \bar{x}_1 .

Equations (2.7) - (2.9) and (2.5a-e) now constitute the governing equations of the problem, with u and u_i being interpreted as dimensionless variables in (2.5a-e). Henceforth we also drop the bar superscripts on the quantities appearing in (2.7) - (2.9), it being understood that these are now dimensionless quantities.

2.4 VARIATIONAL OR WEAK FORMULATION

In order to construct finite element approximations we need to have a weak formulation of the problem. With Ω , Γ , etc. denoting dimensionless regions in \mathbb{R}^2 we define a number of *spaces of functions* which will be required (see, for example, Reddy (1986)). We begin with the Hilbert space $L^2(\Omega)$ of square-integrable functions over Ω . This space is equipped with the inner product and norm

$$(p, q)_0 = \int_{\Omega} pq \, d\Omega \quad \text{and} \quad \|q\|_0 = (q, q)^{\frac{1}{2}},$$

respectively. The Sobolev space $H^1(\Omega)$ is the space of functions which along with first weak derivatives are square-integrable on Ω . That is,

$$H^1(\Omega) = \left\{ v \in L^2(\Omega) : \frac{\partial v}{\partial x_1}, \frac{\partial v}{\partial x_2} \in L^2(\Omega) \right\}.$$

$H^1(\Omega)$ comes equipped with the inner product

$$(u, v)_1 = \int_{\Omega} (uv + \nabla u \cdot \nabla v) \, d\Omega$$

and norm

$$\|v\|_1^2 = \int_{\Omega} v^2 + \left[\frac{\partial v}{\partial x_1} \right]^2 + \left[\frac{\partial v}{\partial x_2} \right]^2 \, d\Omega.$$

Note that $L^2(\Omega)$ is a subspace of $H^1(\Omega)$. We set $\mathbf{X} = H^1(\Omega)^2$ and denote by $V \subset \mathbf{X}$ the space of admissible velocities, defined by

$$V = \{ \mathbf{v} = (v_1, v_2) : v_1, v_2 \in H^1(\Omega) \quad , \\ \mathbf{v} = \mathbf{0} \text{ on } \Gamma_i \cup \Gamma_0 \cup \Gamma_w \quad , \quad v_n = 0 \text{ on } \Gamma_s \cup \Gamma_f \} \quad .$$

That is, V consists of those functions which vanish on the parts of the boundary on which the velocity is prescribed. We also set $Q = L^2(\Omega)$ for the space of admissible pressures.

We now define the bilinear forms $a : \mathbf{X} \times \mathbf{X} \rightarrow \mathbb{R}$ and $b : \mathbf{X} \times Q \rightarrow \mathbb{R}$ by

$$a(\mathbf{u}, \mathbf{v}) = \frac{2}{\text{Re}} \int_{\Omega} \mathbf{D}(\mathbf{u}) \cdot \mathbf{D}(\mathbf{v}) \, d\Omega \quad \text{for all } \mathbf{v}, \mathbf{u} \in \mathbf{X} \quad , \quad (2.10)$$

$$b(\mathbf{v}, q) = - \int_{\Omega} q \, \text{div } \mathbf{v} \, d\Omega \quad \text{for all } \mathbf{v} \in \mathbf{X} \quad (2.11)$$

$$\text{and } q \in Q \quad ,$$

where $\mathbf{D}(\mathbf{u}) \cdot \mathbf{D}(\mathbf{v}) = D_{ij}(\mathbf{u}) D_{ij}(\mathbf{v})$, the trilinear form $c : \mathbf{X} \times \mathbf{X} \times \mathbf{X} \rightarrow \mathbb{R}$ by

$$c(\mathbf{u}, \mathbf{w}, \mathbf{v}) = \int_{\Omega} \rho(\nabla \mathbf{u}) \mathbf{w} \cdot \mathbf{v} \, d\Omega \quad \text{for all } \mathbf{u}, \mathbf{v}, \mathbf{w} \in \mathbf{X} \quad (2.12)$$

where $(\nabla \mathbf{u}) \cdot \mathbf{v} = (\nabla u)_{ij} w_j v_i$, and the linear functional $\ell : \mathbf{X} \rightarrow \mathbb{R}$ by

$$\ell(\mathbf{v}) = \int_{\Omega} \mathbf{f} \cdot \mathbf{v} \, d\Omega \quad \text{for all } \mathbf{v} \in \mathbf{X} \quad . \quad (2.13)$$

Here and henceforth the summation convention on repeated indices is used.

A weak form of the boundary problem may be obtained by taking the scalar product of (2.7) with an arbitrary member $\mathbf{v} \in V$, integrating over the domain Ω and applying the divergence theorem. We have, using also the symmetry of \mathbf{T} ,

$$\begin{aligned} - \int_{\Omega} (\operatorname{div} \mathbf{T}) \cdot \mathbf{v} \, d\Omega &= - \int_{\Gamma} \mathbf{T} \mathbf{n} \cdot \mathbf{v} \, d\Gamma + \int_{\Omega} \mathbf{T} \cdot \nabla \mathbf{v} \, d\Omega \\ &= \int_{\Omega} \mathbf{T} \cdot \mathbf{D}(\mathbf{v}) \, d\Omega - \int_{\Gamma} \mathbf{T} \mathbf{n} \cdot \mathbf{v} \, d\Gamma \end{aligned}$$

so that (2.7) gives

$$\begin{aligned} \int_{\Omega} \mathbf{T}(\mathbf{u}, p) \cdot \mathbf{D}(\mathbf{v}) \, d\Omega + \int_{\Omega} (\nabla \mathbf{u}) \mathbf{u} \cdot \mathbf{v} \, d\Omega - \int_{\Gamma} \mathbf{T} \mathbf{n} \cdot \mathbf{v} \, d\Gamma \\ = \int_{\Omega} \mathbf{f} \cdot \mathbf{v} \, d\Omega \quad . \end{aligned}$$

Using the constitutive equation for \mathbf{T} , the boundary conditions (2.5c-2.5e) and the definition of V , we obtain the equation

$$\begin{aligned} \frac{2}{\text{Re}} \int_{\Omega} \mathbf{D}(\mathbf{u}) \cdot \mathbf{D}(\mathbf{v}) \, d\Omega - \int_{\Omega} p \, \text{div} \, \mathbf{v} \, d\Omega + \int_{\Omega} (\nabla \mathbf{u}) \mathbf{u} \cdot \mathbf{v} \, d\Omega \\ = \int_{\Omega} \mathbf{v} \cdot \mathbf{f} \, d\Omega \quad \text{for all } \mathbf{v} \in V \quad . \end{aligned} \quad (2.14)$$

Using the definitions (2.10) - (2.13) we may write (2.14) in the form

$$a(\mathbf{u}, \mathbf{v}) + b(\mathbf{v}, p) + c(\mathbf{u}, \mathbf{u}, \mathbf{v}) = \ell(\mathbf{v}) \quad . \quad (2.15)$$

Rather than involve the incompressibility condition exactly, it will be convenient from a computational point of view to perturb this constraint by replacing (2.8) with the condition

$$\epsilon p + \text{div} \, \mathbf{u} = 0 \quad , \quad (2.16)$$

where ϵ is a small penalty parameter. Thus (2.16) amounts to a condition of small compressibility which approaches the incompressible limit as $\epsilon \rightarrow 0$ (Carey and Oden (1982)).

If we now multiply (2.16) by arbitrary $q \in Q$ and integrate we obtain the equation

$$\epsilon \int_{\Omega} pq \, d\Omega + \int_{\Omega} q \, \text{div} \, \mathbf{u} = 0$$

or

$$- \epsilon(p, q)_0 + b(q, u) = 0 \quad . \quad (2.17)$$

Equation (2.16) may be used to eliminate the pressure by substituting in (2.14), to get

$$\begin{aligned} \frac{2}{\text{Re}} \int_{\Omega} \mathbf{D}(\mathbf{u}) \cdot \mathbf{D}(\mathbf{v}) \, d\Omega + \int_{\Omega} \frac{1}{\epsilon} (\text{div } \mathbf{u}) \cdot (\text{div } \mathbf{v}) \, d\Omega + \int_{\Omega} (\nabla \mathbf{u}) \mathbf{u} \cdot \mathbf{v} \, d\Omega \\ = \int_{\Omega} \mathbf{v} \cdot \mathbf{f} \, d\Omega \quad \text{for all } \mathbf{v} \in V \quad . \end{aligned}$$

For f given or fixed we may now define the following *auxiliary* problem

(A): Given f on Ω , \mathbf{u}_i on Γ_i and a function \mathbf{U}_i on Ω which satisfies $\mathbf{U}_i = \mathbf{u}_i$ on Γ_i , find \mathbf{u} and p such that $\mathbf{u} - \mathbf{U}_i \in V$, $p \in Q$, and which satisfy (2.15) and (2.17) for all $\mathbf{v} \in V$, $q \in Q$.

2.5 THE NORMAL STRESS EQUATION

We still have to deal with the free surface equation (2.9) for the normal stress. Since this is implicitly a nonlinear ordinary differential equation for f , it has to be supplemented by two boundary conditions on f . We take these to be the conditions corresponding to the problem in Figure 2.1, that is, $f(0) = 1$ and $f'(1) = L$ (recall that x and f are now dimensionless). That is, the

height of the surface is prescribed at $x_1 = 0$ and its slope is given at $x_1 = L$. Other possible combinations are easily accommodated as required. To obtain a variational formulation of (2.9) we define

$$G = \{g \in L^2(0,1) : g(L) = 0\} \quad ;$$

that is, G represents the space of functions to which the *slope* $f' \equiv h$ will be required to belong. Now multiplying (2.9) by an arbitrary $g \in G$, integrating over the free surface Γ_f and using (2.6), we get

$$\frac{Re^2}{S} \int_0^L \mathbf{Tn}(h) \cdot \mathbf{n}(h) g \, dx_1 = \int_0^L \left\{ \left[\frac{h}{\sqrt{1+h^2}} \right]' g + a \left[\frac{g}{f\sqrt{1+h^2}} \right] \right\} dx_1$$

where again $a = 0$ for a plane problem and $a = 1$ for an axisymmetric problem. The normal $\mathbf{n}(h)$ is given as a function of h by

$$\mathbf{n} = \frac{(-h, 1)}{\sqrt{1+h^2}} \quad . \quad (2.18)$$

The first term on the right-hand side becomes

$$\int_0^L \left[\frac{h}{\sqrt{1+h^2}} \right]' g \, dx_1 = \left. \frac{gh}{\sqrt{1+h^2}} \right|_0^L - \int_0^L \frac{hg'}{\sqrt{1+h^2}} \, dx_1$$

so that

$$\begin{aligned} & \left. \frac{gh}{\sqrt{1+h^2}} \right|_0^L - \int_0^L \frac{hg'}{\sqrt{1+h^2}} dx_1 + a \int_0^L \frac{g}{f\sqrt{1+h^2}} dx_1 \\ &= \frac{Re^2}{S} \int_0^L \mathbf{Tn}(h) \cdot \mathbf{n}(h) g dx_1 \quad . \end{aligned}$$

For axisymmetric problems it will be necessary to make some assumption about f in the term containing a , in order to solve for h . For example, in the $(n+1)$ th iteration of an iterative solution procedure we may set $f = f^{(n)}$. Assuming that such assumption has been made the *variational normal stress problem* is

(N) : given u and p , find $h \in G$ such that

$$\begin{aligned} & \frac{Re^2}{S} \int_0^1 \mathbf{T}(u, p) \mathbf{n}(h) \cdot \mathbf{n}(h) g dx_1 + \int_0^1 \frac{hg'}{\sqrt{1+h^2}} dx_1 \\ & - a \int_0^1 \frac{g}{f\sqrt{1+h^2}} g dx_1 + \frac{h(0)G(0)}{\sqrt{1+h^2(0)}} = 0 \end{aligned}$$

for all $g \in G$.

(2.19)

CHAPTER 3

FINITE ELEMENT APPROXIMATIONS

3.1 THE AUXILIARY PROBLEM

In Chapter 2 we formulated the penalised auxiliary problem (A) involving the Navier-Stokes equations, in the form: find \mathbf{u} and p such that $\mathbf{u} - \mathbf{U}_i \in V$ and $p \in Q$, and such that

$$a(\mathbf{u}, \mathbf{v}) + b(\mathbf{v}, p) + c(\mathbf{u}, \mathbf{u}, \mathbf{v}) = \ell(\mathbf{v}) \quad \text{for all } \mathbf{v} \in V, \quad (3.1)$$

$$-\epsilon(p, q) + b(\mathbf{u}, q) = 0 \quad \text{for all } q \in Q. \quad (3.2)$$

Here it is assumed that the free surface is known. It is difficult to solve (3.1) and (3.2) in closed form since the spaces of admissible functions V and Q are infinite-dimensional: we have

$$V = \text{span}\{\theta_i\}_{i=1}^{\infty}$$

$$Q = \text{span}\{\chi_i\}_{i=1}^{\infty}$$

where $\{\theta_i\}_{i=1}^{\infty}$ and $\{\chi_i\}_{i=1}^{\infty}$ are bases for V and Q respectively.

The Galerkin method is a method for constructing approximate solutions to variational problems such as (3.1) and (3.2) in finite-dimensional subspaces of V and Q . Instead of posing the problem in V and Q we define spaces V^h and Q^h spanned by a finite number of linearly independent basis functions $\{\theta_i\}$ and $\{\chi_i\}$. That is,

$$V^h = \text{span}\{\theta_i\}_{i=1}^N, \quad V^h \subset V, \quad ,$$

$$Q^h = \text{span}\{\chi_i\}_{i=1}^M, \quad Q^h \subset Q. \quad .$$

In the case of finite elements h is the mesh parameter that lies between 0 and 1, and is a measure of how close V^h and Q^h are to V and Q . The approximate problem follows from (3.1) and (3.2), and is: find u_h and p_h such that $u_h - U_h \in V^h$, $p_h \in Q^h$, and

$$a(u_h, v_h) + b(v_h, p_h) + c(u_h, u_h, v_h) = \ell(v_h) \quad \text{for all } v_h \in V_h, \quad (3.3)$$

$$- \epsilon(p_h, q_h) + b(u_h, q_h) = 0 \quad \text{for all } q_h \in Q_h, \quad (3.4)$$

where U_h is a suitable approximation to U_i .

Finite element formulations of the form (3.3) and (3.4) are called *mixed finite element methods* since two different spaces are involved, i.e. V^h and Q^h .

In the general Galerkin method there is no systematic way of constructing reasonable basis functions. A poor choice may produce ill-conditioned element matrices resulting in inaccurate solutions. These difficulties can be overcome by using the finite element method, which is a special case of the Galerkin method. In the finite element method the basis functions are generated in a systematic manner in such a way that families of spaces V^h and Q^h defined by the finite element procedure have the property that V^h , Q^h approach V , Q as h approaches zero.

In Section 3.2 we construct a finite element mesh representing Ω with piecewise-polynomial basis functions defined on the mesh, which generate the finite-dimensional subspaces of V and Q . We consider its application to both two- and one-dimensional problems and include discussion of the use of master elements.

Then in Section 3.3 we consider in more detail the approximation of the plane and axisymmetric Navier-Stokes equations. We will then describe in detail the construction of element stiffness matrices. We also show how the free surface stresses are obtained from the solution of the discrete form of the auxiliary problem.

In Section 3.4 we briefly show how numerical integration is used in the finite element calculations. In Section 3.5 we describe the finite element calculations required to solve the one-dimensional normal stress problem formulated on the free surface in Chapter 2.

In Section 3.6 we discuss how stresses are extrapolated for use on the free boundary, in the solution of the normal stress equation. Finally, in Section 3.7 the discrete form of the normal stress equation is presented.

3.2 FINITE ELEMENT APPROXIMATIONS

The finite element method is a technique for constructing approximate solutions to variational boundary value problems. The method involves dividing the domain of the problem into a finite number of sub-domains, the finite elements, and constructing an approximation of the solution over the collection of finite elements. The basis functions are defined piecewise over the finite elements and are chosen to be low-order polynomials. To construct the piecewise basis functions, we first partition the domain Ω of the problem into a finite number E of sub-domains $\Omega_1, \Omega_2, \dots, \Omega_E$ called finite elements which satisfy

$$\Omega_b \cup \Omega_c \neq \emptyset \text{ for } b \neq c \text{ and } \bigcup_{e=1}^E \Omega_e = \bar{\Omega} .$$

Nodal points x_1, \dots, x_G are allocated at least at the vertices of elements (see Figure 3.1).

The set of elements and nodes that make up the domain is called a finite element mesh. For the Navier-Stokes problem we will make use

of *nine-noded quadrilateral elements*, the nine nodes being required for approximation of the velocities by biquadratic functions.

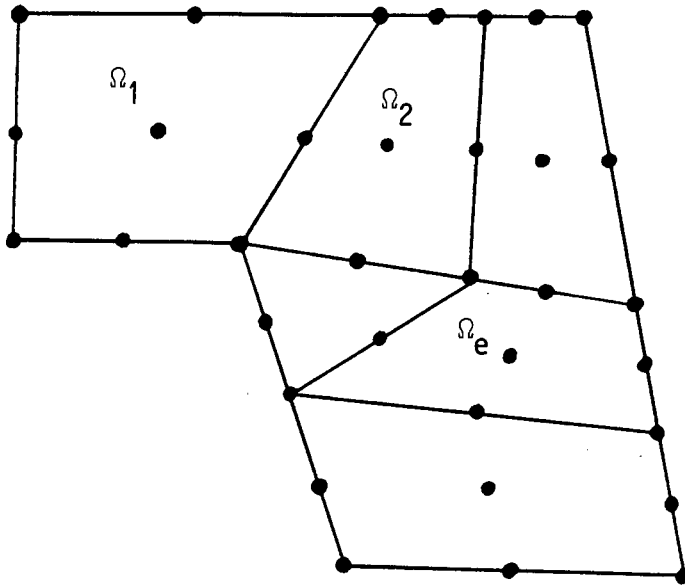


Figure 3.1 : Example of a finite element mesh

The global basis functions θ_i are required to satisfy the following properties:

- (i) θ_i is continuous;
- (ii) θ_i is non-zero only on those elements connected to node i ;
- (iii) $\theta_i(x_j) = \begin{cases} 1 & \text{if } i = j \\ 0 & \text{otherwise} \end{cases}$;
- (iv) the restriction $\theta_i^{(e)} = \theta_i|_{\Omega_e}$ of θ_i to Ω_e is a *polynomial*.

It follows that on Ω_e we may write

$$\mathbf{u}_h^{(e)} \equiv \mathbf{u}_h \Big|_{\Omega_e} = \sum_{A=1}^9 \mathbf{a}_A^{(e)} \theta_A^{(e)},$$

$$\mathbf{v}_h^{(e)} \equiv \mathbf{v}_h \Big|_{\Omega_e} = \sum_{A=1}^9 \mathbf{b}_A^{(e)} \theta_A^{(e)},$$

and that $\mathbf{a}_A^{(e)}$ and $\mathbf{b}_A^{(e)}$ are respectively the *nodal values* of $\mathbf{u}_h^{(e)}$ and $\mathbf{v}_h^{(e)}$.

Consider now the term $a(\mathbf{u}_h, \mathbf{v}_h)$ in (3.1). We have

$$a(\mathbf{u}_h, \mathbf{v}_h) = \sum_{e=1}^E \underbrace{\frac{2}{\text{Re}} \int_{\Omega_e} \mathbf{D}(\mathbf{u}_h^{(e)}) \cdot \mathbf{D}(\mathbf{v}_h^{(e)}) \, d\Omega_e}_{\mathbf{a}^{(e)}(\mathbf{u}_h^{(e)}, \mathbf{v}_h^{(e)})}, \quad (3.5)$$

so that if we write \mathbf{D} in vector form as

$$\mathbf{D}(\mathbf{u}) = \begin{bmatrix} D_{11} \\ D_{22} \\ 2D_{12} \\ D_{33} \end{bmatrix} = \begin{bmatrix} \partial u_1 / \partial x_1 \\ \partial u_2 / \partial x_2 \\ \partial u_1 / \partial x_2 + \partial u_2 / \partial x_1 \\ \alpha u_2 / x_2 \end{bmatrix},$$

then

$$\mathbf{D}(\mathbf{u}_h^{(e)}) = \mathbf{B}^{(e)} \mathbf{a}^{(e)} = \sum_{A=1}^9 \mathbf{B}_A^{(e)} \mathbf{a}_A^{(e)} \quad (3.6)$$

with a similar expression for $\mathbf{D}(\mathbf{v}_h^{(e)})$, where

$$\mathbf{B}_A^{(e)} = \begin{bmatrix} \partial \theta_A^{(e)} / \partial x_1 & 0 \\ 0 & \partial \theta_A^{(e)} / \partial x_2 \\ \partial \theta_A^{(e)} / \partial x_2 & \partial \theta_A^{(e)} / \partial x_1 \\ 0 & \alpha \theta_A^{(e)} / x_2 \end{bmatrix}$$

and $\mathbf{a}^{(e)\text{T}} = [\mathbf{a}_1^{(e)\text{T}} \dots \mathbf{a}_9^{(e)\text{T}}]$. Substituting in (3.5) we obtain

$$\mathbf{a}^{(e)}(\mathbf{u}_h^{(e)}, \mathbf{v}_h^{(e)}) = \mathbf{b}^{(e)\text{T}} \mathbf{K}^{(e)} \mathbf{a}^{(e)}$$

where

$$\mathbf{K}^{(e)} = \frac{2}{\text{Re}} \int_{\Omega_e} \mathbf{B}^{(e)\text{T}} \mathbf{B}^{(e)} d\Omega_e \quad (3.7)$$

We consider next the term

$$c(\mathbf{u}_h, \mathbf{u}_h, \mathbf{v}_h) = \sum_{e=1}^E c^{(e)}(\mathbf{u}_h^{(e)}, \mathbf{u}_h^{(e)}, \mathbf{v}_h^{(e)})$$

where

$$c^{(e)}(\mathbf{u}_h^{(e)}, \mathbf{u}_h^{(e)}, \mathbf{v}_h^{(e)}) = \int_{\Omega_e} (\nabla \mathbf{u}_h^{(e)}) \mathbf{u}_h^{(e)} \cdot \mathbf{v}_h^{(e)} d\Omega_e .$$

Since this is a nonlinear term we will linearise it in the solution algorithm by making an assumption about $\mathbf{u}_h^{(e)}$ in the first slot (see later, Chapter 4). Suppose that this (known) function is denoted by $\mathbf{w}_h^{(e)}$. Then we write

$$\begin{aligned} (\nabla \mathbf{w}_h^{(e)}) \mathbf{u}_h^{(e)} &= \mathbf{C}^{(e)} \mathbf{a}^{(e)} \\ &= \sum_{A=1}^9 \mathbf{C}_A^{(e)} \mathbf{a}_A^{(e)} \end{aligned}$$

where the matrix $\mathbf{C}_A^{(e)}$ is given by

$$[\mathbf{C}_A]_{ij}^{(e)} = \sum_{B=1}^9 c_{iB}^{(e)} \theta_{B,j}^{(e)} \theta_A^{(e)} ;$$

here we have written $\mathbf{w}_h^{(e)} = \sum_{A=1}^9 \mathbf{c}_A^{(e)} \theta_A^{(e)}$. Thus

$$c^{(e)}(\mathbf{w}_h^{(e)}, \mathbf{u}_h^{(e)}, \mathbf{v}_h) = \mathbf{b}^{(e)T} \mathbf{L}^{(e)} \mathbf{a}^{(e)}$$

where

$$\mathbf{L}^{(e)} = \int_{\Omega_e} \mathbf{B}^{(e)\top} \mathbf{C}^{(e)} d\Omega_e .$$

To make further progress we now have to construct the basis functions χ_i for Q^h . We define Q^h to be the space of functions, *not necessarily continuous*, whose restrictions to Ω_e are linear. Thus

$$p_h^{(e)} \equiv p_h \Big|_{\Omega_e} = \sum_{A=1}^3 a_A^{(e)} \chi_A^{(e)} = \mathbf{a}^{(e)\top} \boldsymbol{\chi}^{(e)} ,$$

$$q_h^{(e)} = q_h \Big|_{\Omega_e} = \sum_{A=1}^3 \beta_A^{(e)} \chi_A^{(e)} = \boldsymbol{\beta}^{(e)\top} \boldsymbol{\chi}^{(e)} ,$$

where $\chi_1^{(e)} = 1$, $\chi_2^{(e)} = x_1$, $\chi_3^{(e)} = x_2$. The coefficients $a_i^{(e)}$ and $\beta_i^{(e)}$ are not associated with nodal points.

The combination of a nine-noded biquadratic element for velocity with a discontinuous linear element for pressure has been shown to be unconditionally stable and convergent (Carey and Oden (1982)).

We thus have

$$b(\mathbf{u}_h, \mathbf{q}_h) = \sum_{e=1}^E b^{(e)}(\mathbf{u}_h^{(e)}, \mathbf{q}_h^{(e)})$$

where

$$\mathbf{b}^{(e)}(\mathbf{u}_h^{(e)}, \mathbf{q}_h^{(e)}) = -\boldsymbol{\beta}^{(e)} \mathbf{T}_N^{(e)} \mathbf{a}^{(e)} \quad (3.9)$$

and the matrix $\mathbf{N}^{(e)}$ is given by

$$\mathbf{N}^{(e)} = - \int_{\Omega_e} \chi^{(e)} \mathbf{T}_E^{(e)} d\Omega_e ,$$

where the row vector $\mathbf{E}^{(e)}$ arises from the expression (see (3.6))

$$\begin{aligned} \operatorname{div} \mathbf{u}_h^{(e)} &= \sum_{j=1}^3 \mathbf{B}_{1j}^{(e)} a_j^{(e)} + \mathbf{B}_{2j}^{(e)} a_j^{(e)} + \mathbf{B}_{4j}^{(e)} a_j^{(e)} \\ &\equiv \mathbf{E}^{(e)} \mathbf{a}^{(e)} . \end{aligned}$$

Similarly we have

$$\mathbf{b}(\mathbf{v}_h^{(e)}, \mathbf{p}_h) = -\mathbf{b}^{(e)} \mathbf{T}_N^{(e)} \mathbf{a}^{(e)} . \quad (3.10)$$

Finally,

$$(\mathbf{p}_h, \mathbf{q}_h)_0 = \sum_{e=1}^E (\mathbf{p}_h^{(e)}, \mathbf{q}_h^{(e)})_{0,e}$$

Since the pressures are discontinuous the quantities $\mathbf{a}^{(e)}$ are easily condensed out at element level since \mathbf{H} has the form

$$\mathbf{H} = \begin{bmatrix} \mathbf{H}^{(1)} & 0 & 0 & \dots & \dots \\ 0 & \mathbf{H}^{(2)} & 0 & \dots & \dots \\ & & & & \\ & & & & \\ & & & & \\ & & & & \\ & & & & \\ & & & & \\ & & & & \\ & & & & \mathbf{H}^{(E)} \end{bmatrix}$$

where $\mathbf{H}^{(e)}$ are 3×3 matrices.

3.3 CALCULATION OF ELEMENT MATRICES

Instead of defining local basis functions for each element, we can set up a master element $\hat{\Omega}$ which is not part of the actual finite element mesh and which has its own coordinate system. We choose $\hat{\Omega}$ to be the square $(-1,1) \times (-1,1)$ as shown in Figure 3.2.

The master element has the same system of nodal points as the elements Ω_e in the actual mesh. An invertible transformation is used to map points from the master element onto points in each element, as shown in Figure 3.2. We introduce a map T_e of $\hat{\Omega}$ onto Ω_e by

$$T_e : \hat{\Omega} \rightarrow \Omega_e \quad ,$$

$$T_e \xi = \mathbf{x} \quad \text{or} \quad \begin{bmatrix} \mathbf{x} \\ \mathbf{y} \end{bmatrix} = \begin{bmatrix} \mathbf{x}(\xi, \eta) \\ \mathbf{y}(\xi, \eta) \end{bmatrix} \quad . \quad (3.14)$$

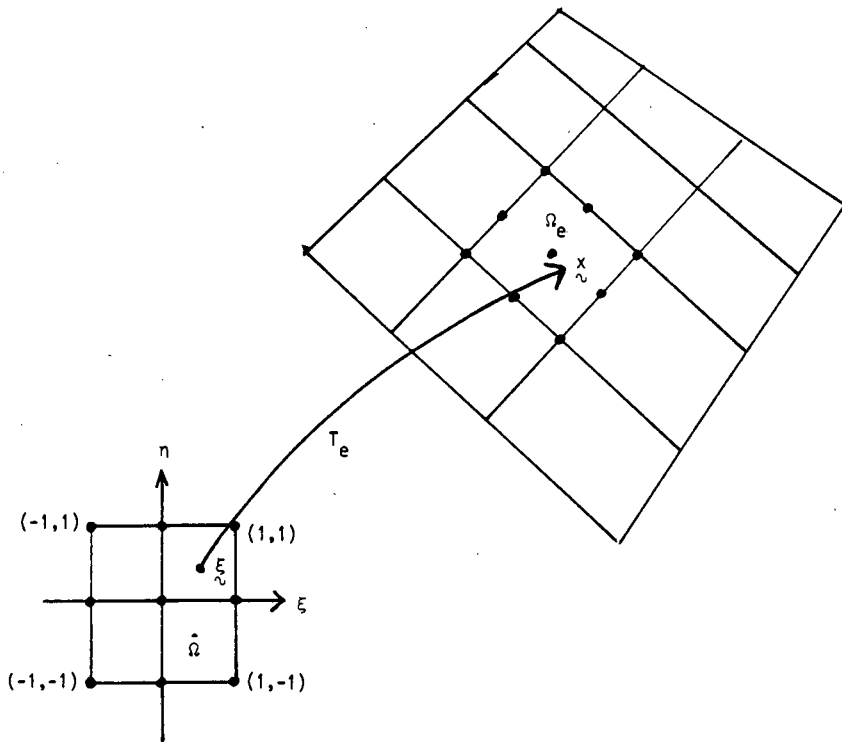


Figure 3.2 : The master element $\hat{\Omega}$ and map T_e to Ω_e

Now we can define the local basis functions $\hat{\theta}_A$ on $\hat{\Omega}$ and use (3.14) to map $\hat{\theta}_A$ to $\theta_A^{(e)}$ by defining $\theta_A^{(e)}$ to be functions on Ω_e satisfying

$$\theta_A^{(e)}(x,y) = \hat{\theta}_A(\xi(x,y), \eta(x,y)) \quad . \quad (3.15)$$

For the velocities the local basis functions corresponding to the nine-noded element are (with numbering as in Figure 3.2)

$$\hat{\theta}_1 = \frac{1}{4} \xi(\xi - 1)(\eta^2 - \eta)$$

$$\hat{\theta}_2 = \frac{1}{2} \eta(1 - \xi)(\eta - 1)$$

$$\hat{\theta}_3 = \frac{1}{4} \xi\eta(\xi + 1)(\eta - 1)$$

$$\begin{aligned}
\hat{\theta}_4 &= \frac{1}{2} \xi(\xi + 1)(1 - \eta) \\
\hat{\theta}_5 &= \frac{1}{4} \xi\eta(\xi + 1)(\eta + 1) \\
\hat{\theta}_6 &= \frac{1}{2} \eta(1 - \xi)(\eta + 1) \\
\hat{\theta}_7 &= \frac{1}{4} \xi\eta(\xi - 1)(\eta + 1) \\
\hat{\theta}_8 &= \frac{1}{2} \xi(\xi - 1)(1 - \eta) \\
\hat{\theta}_9 &= (1 - \xi^2)(1 - \eta^2) \quad .
\end{aligned} \tag{3.16}$$

It is now possible to transform operations on a finite element Ω_e to the master element. The complete finite element mesh containing E elements is generated by a sequence of transformations $\{T_1, T_2, \dots, T_E\}$ in which each element Ω_e is the image of the master element under a coordinate map T_e , as shown in Figure 3.2.

The map T_e can be constructed using the finite element local basis functions, that is,

$$\begin{aligned}
x(\xi, \eta) &= \sum_{A=1}^9 \hat{\theta}_A(\xi, \eta) x_A^{(e)} \quad , \\
y(\xi, \eta) &= \sum_{A=1}^9 \hat{\theta}_A(\xi, \eta) y_A^{(e)} \quad ,
\end{aligned} \tag{3.17}$$

where $x^{(e)}$ and $y^{(e)}$ are the coordinates of the nodal points of Ω_e . For the axisymmetric case x and y are replaced by z and r .

The velocity $\mathbf{u}^{(e)}$ on Ω_e can now be expressed in the form

$$\mathbf{u}^{(e)}(\mathbf{x}(\xi, \eta)) = \sum_{A=1}^9 \hat{\phi}_A(\xi, \eta) \mathbf{a}_A^{(e)} \quad (3.18)$$

where $\mathbf{a}_A^{(e)}$ is the value of $\mathbf{u}^{(e)}$ at node A (with appropriate numbering at local level).

It follows now that all the matrices defined in Section 3.2 can be evaluated on $\hat{\Omega}$ by using the transformation (3.17). We proceed to show how this is done. First, since T_e is by definition invertible the relations

$$\begin{aligned} T_e^{-1} : \Omega_e \rightarrow \hat{\Omega} \quad , \quad \xi &= \xi(x, y) \quad , \\ \eta &= \eta(x, y) \quad , \end{aligned} \quad (3.19)$$

exist. To obtain the derivatives $\frac{\partial}{\partial x}$ and $\frac{\partial}{\partial y}$ in terms of $\frac{\partial}{\partial \xi}$ and $\frac{\partial}{\partial \eta}$ we use the chain rule in the form

$$\left. \begin{aligned} \frac{\partial}{\partial x} &= \frac{\partial \xi}{\partial x} \frac{\partial}{\partial \xi} + \frac{\partial \eta}{\partial x} \frac{\partial}{\partial \eta} \\ \frac{\partial}{\partial y} &= \frac{\partial \xi}{\partial y} \frac{\partial}{\partial \xi} + \frac{\partial \eta}{\partial y} \frac{\partial}{\partial \eta} \end{aligned} \right\} \quad (3.20)$$

or, in matrix form,

$$\begin{bmatrix} \frac{\partial}{\partial \xi} \\ \frac{\partial}{\partial \eta} \end{bmatrix} = \begin{bmatrix} \frac{\partial x}{\partial \xi} & \frac{\partial y}{\partial \xi} \\ \frac{\partial x}{\partial \eta} & \frac{\partial y}{\partial \eta} \end{bmatrix} \begin{bmatrix} \frac{\partial}{\partial x} \\ \frac{\partial}{\partial y} \end{bmatrix} \quad (3.21)$$

Solving for $\frac{\partial}{\partial x}$ and $\frac{\partial}{\partial y}$ we get

$$\begin{bmatrix} \frac{\partial}{\partial x} \\ \frac{\partial}{\partial y} \end{bmatrix} = J^{-1} \begin{bmatrix} \frac{\partial y}{\partial \eta} & -\frac{\partial x}{\partial \eta} \\ -\frac{\partial y}{\partial \xi} & \frac{\partial x}{\partial \xi} \end{bmatrix} \begin{bmatrix} \frac{\partial}{\partial \xi} \\ \frac{\partial}{\partial \eta} \end{bmatrix} \quad (3.22)$$

where J , the jacobian, is the determinant of the matrix in (3.21).

We now return to the problem of evaluating the integrals in Section 3.2. First, the local basis functions $\hat{\theta}_A^{(e)}$ are obtained from $\hat{\theta}_A$ by (3.15). Next, derivatives of the local basis functions are obtained from

$$\frac{\partial \hat{\theta}_A^{(e)}}{\partial x} = \frac{\partial \hat{\theta}_A}{\partial \xi} \frac{\partial \xi}{\partial x} + \frac{\partial \hat{\theta}_A}{\partial \eta} \frac{\partial \eta}{\partial x} \quad (3.23)$$

and

$$\frac{\partial \hat{\theta}_A^{(e)}}{\partial y} = \frac{\partial \hat{\theta}_A}{\partial \xi} \frac{\partial \xi}{\partial y} + \frac{\partial \hat{\theta}_A}{\partial \eta} \frac{\partial \eta}{\partial y} \quad (3.24)$$

According to (3.17),

$$\frac{\partial x}{\partial \xi} = \sum_{A=1}^9 x_A \frac{\partial \hat{\theta}_A}{\partial \xi} \quad (3.25)$$

with similar expressions for the other derivatives. We thus obtain

$$\begin{bmatrix} \frac{\partial \hat{\theta}_B^{(e)}}{\partial x} \\ \\ \\ \\ \\ \\ \frac{\partial \hat{\theta}_B^{(e)}}{\partial y} \end{bmatrix} = \frac{1}{J} \begin{bmatrix} \Sigma_A y_A \frac{\partial \hat{\theta}_A}{\partial \eta} & -\Sigma_A y_A \frac{\partial \hat{\theta}_A}{\partial \xi} \\ \\ \\ \\ -\Sigma_A x_A \frac{\partial \hat{\theta}_A}{\partial \eta} & \Sigma_A x_A \frac{\partial \hat{\theta}_A}{\partial \xi} \end{bmatrix} \begin{bmatrix} \frac{\partial \hat{\theta}_B^{(e)}}{\partial \xi} \\ \\ \\ \\ \frac{\partial \hat{\theta}_B^{(e)}}{\partial \eta} \end{bmatrix}$$

Using these results, all the integrals over Ω_e may be carried over by calculations defined only on the master element $\hat{\Omega}$.

3.4 NUMERICAL INTEGRATION

The integrals appearing in Section 3.2 are evaluated on the master element $\hat{\Omega}$. Thus a typical integral will be of the form

$$\int_{\Omega_e} g^{(e)}(x,y) dx dy = \int_{\hat{\Omega}} \hat{g}(\xi,\eta) |J(\xi,\eta)| d\xi d\eta .$$

In the actual calculations Gaussian quadrature is used to evaluate the integrals. For a function of a single variable integrated over the interval $[-1,1]$ the Gaussian quadrature rule is

$$\int_{-1}^1 \hat{G}(\xi) d\xi = \sum_{K=1}^{NG} \hat{G}(\xi_K) w_K + \hat{E}$$

where $\xi_K (K=1, \dots, NG)$ are the sampling points, w_K are quadrature weights, and NG is the order of the quadrature rule. If \hat{G} is a polynomial, then NG can be chosen large enough so that the error \hat{E} is zero. Specifically, a polynomial of degree $(2n-1)$ in ξ is integrated exactly by a one-dimensional rule of order n . We construct a two-dimensional rule as a tensor product of one-dimensional rules, so



that for an integral over the master element $\hat{\Omega}$ we have the rule

$$\int_{\hat{\Omega}} \hat{G}(\xi, \eta) d\xi d\eta = \int_{-1}^1 \int_{-1}^1 \hat{G}(\xi, \eta) d\xi d\eta$$

$$\approx \sum_{K=1}^{NG} \sum_{L=1}^{NG} \hat{G}(\xi_K, \eta_L) w_K w_L \quad (3.26)$$

Table 3.1 gives details of rules of order 2 and 3, for the one-dimensional case. The two-dimensional rules then follow directly according to (3.26).

Table 3.1

NG	ξ_K	w_K	
2	$\pm \frac{1}{\sqrt{3}}$	1	
3	$\pm \sqrt{3/5}$	5/9	
	0	8/9	

3.5 THE NORMAL STRESS EQUATION

We discuss in this Section the procedure for approximating the normal stress equation by finite elements. Recall from (2.19) that this

equation in variational form is

$$\frac{\text{Re}^2}{S} \int_0^L \mathbf{T}(\mathbf{u}, p) \mathbf{n}(h) \cdot \mathbf{n}(h) g \, dx_1 + \int_0^L \frac{hg'}{\sqrt{1+h^2}} \, dx_1$$

$$- a \int_0^L \frac{g}{f\sqrt{1+h^2}} \, dx_1 + \frac{h(0)G(0)}{\sqrt{1+h^2(0)}} = 0$$

for all $g \in G$.

(3.27)

The stress is obtained from the velocity and pressure in the predictor phase of the algorithm, that is, from the auxiliary problem, and is substituted into (3.27). Also, for the case of axisymmetry a term involving f appears in (3.27); this is assumed to be given by the function f in the previous iteration.

The one-dimensional domain on which the normal stress equation is defined is divided into finite elements in such a way as to be compatible with the mesh used for the Navier-Stokes equations (see Figure 3.3).

Specifically, the mesh comprises elements $w_e (e=1, \dots, \bar{E})$, as indicated in Figure 3.3. As in the case of the Navier-Stokes equations calculations are carried out on a master element $\hat{w} = [-1, 1]$. The slope h is approximated by a continuous, piecewise

quadratic function so that we have, on ω_e ,

$$x^{(e)} = \sum_{A=1}^3 x_A^{(e)} \hat{\psi}_A(\xi)$$

where the local basis functions are given by

$$\left. \begin{aligned} \hat{\psi}_1(\xi) &= \frac{1}{2} \xi(\xi - 1) \\ \hat{\psi}_2(\xi) &= (1 + \xi)(1 - \xi) \\ \hat{\psi}_3(\xi) &= \frac{1}{2} \xi(\xi + 1) \end{aligned} \right\} \quad (3.28)$$

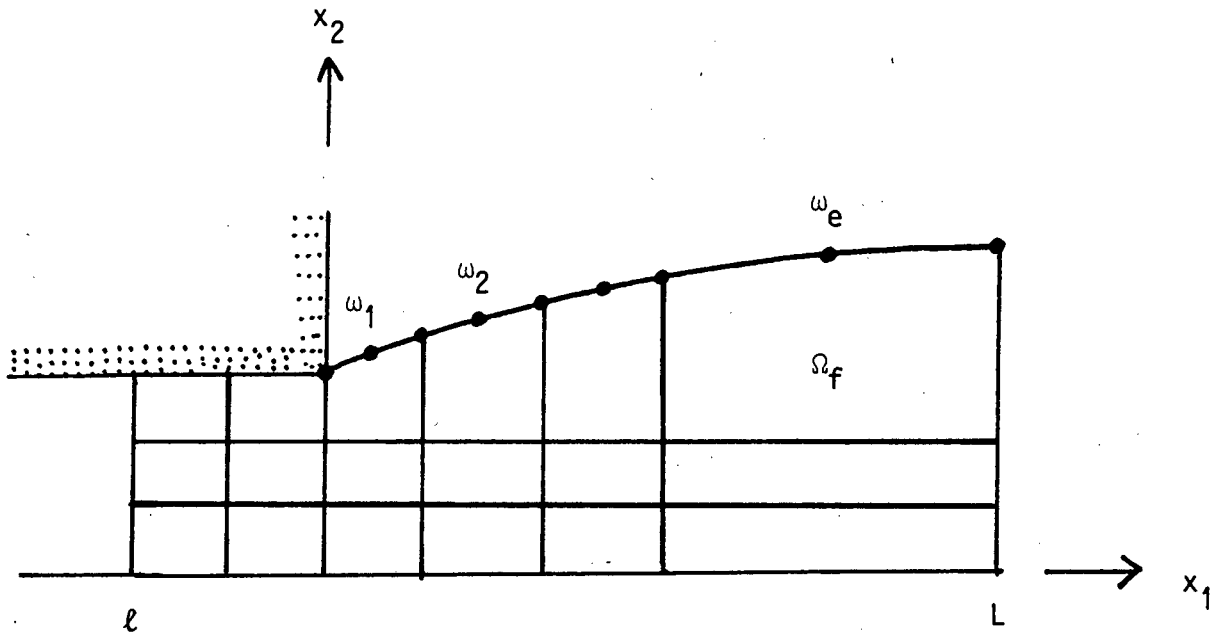


Figure 3.3 : Finite element mesh on the free boundary, corresponding to mesh in the interior of the domain

We now write, on element ω_e ,

$$h^{(e)}(x(\xi)) = \sum_{A=1}^3 h_A^{(e)} \hat{\psi}_A(\xi)$$

where $h_A^{(e)}$ are the nodal values of h on ω_e .

Before proceeding further it is necessary to describe exactly how the stress in (3.27) is found on ω_e from the known values of u_h and p_h on the element Ω_f (see Figure 3.3). To carry out the integrations over ω_e or $\hat{\omega}$ we require the stress at the integration points.

3.6 STRESS EXTRAPOLATION

The values of stress at the integration points in Ω_f are regarded as optimal, and the stress along ω_e is obtained by extrapolation through a linear least-squares fit. The procedure is described in detail in Burnett (1987) (Section 13.3) for the case in which nodal values are required; we now describe its implementation for the problem at hand.

Let \mathbf{T}_{ij}^{Ω} denote the vector of T_{ij} evaluated at the gauss points in Ω_f or $\hat{\Omega}$. That is, with reference to a master element $\hat{\Omega}$,

$$\mathbf{T}_{ij}^{\Omega} = \begin{bmatrix} T_{ij}(\xi_1, \eta_1) \\ \vdots \\ T_{ij}(\xi_4, \eta_4) \end{bmatrix}$$

where (ξ_A, η_A) are the integration points corresponding to the 2×2 rule. We are interested in four such vectors: \mathbf{T}_{11}^Ω , \mathbf{T}_{22}^Ω , \mathbf{T}_{12}^Ω and \mathbf{T}_{33}^Ω (the last only for the case of axisymmetry). Similarly, let \mathbf{T}_{ij}^ω be the 3×1 vector of values of T_{ij} at the three integration points on ω_e or $\hat{\omega}$.

We do a linear least-squares fit to \mathbf{T}_{ij}^Ω so that the values of T_{ij} at the integration points on ω_e are approximated by a linear polynomial p_{ij} , where

$$p_{ij}(\xi, \eta) = a_{ij} + b_{ij}\xi + c_{ij}\eta$$

on the master element. Thus the vector \mathbf{T}_{ij}^ω of stresses at integration points on ω_e is found from

$$\begin{bmatrix} T_{ij}(-1/\sqrt{3}, 1) \\ T_{ij}(0, 1) \\ T_{ij}(+1/\sqrt{3}, 1) \end{bmatrix} = \begin{bmatrix} 1 & -1/\sqrt{3} & 1 \\ 1 & 0 & 1 \\ 1 & +1/\sqrt{3} & 1 \end{bmatrix} \begin{bmatrix} a_{ij} \\ b_{ij} \\ c_{ij} \end{bmatrix}$$

$$\text{or } \mathbf{T}_{ij}^\omega = \mathbf{R} \mathbf{a}_{ij} \quad (3.29)$$

The coefficients a_{ij} , b_{ij} and c_{ij} are obtained by minimising the error, that is, by minimising

$$E(a_{ij}, b_{ij}, c_{ij}) = \sum_{A=1}^4 [a_{ij} + b_{ij}\xi_A + c_{ij}\eta_A - T_{ij}^{\Omega}(\xi_A, \eta_A)]^2$$

for $(i,j) = (1,1), (2,2), (1,2)$ and $(3,3)$. A necessary condition for a minimum is that

$$\frac{\partial E}{\partial a_{ij}} = 0, \quad \frac{\partial E}{\partial b_{ij}} = 0, \quad \frac{\partial E}{\partial c_{ij}} = 0,$$

which yields the set of linear equations

$$\mathbf{P} \mathbf{a}_{ij} = \mathbf{Q} \mathbf{T}_{ij}^{\Omega};$$

here the matrices \mathbf{P} and \mathbf{Q} are given by

$$\mathbf{P} = \begin{bmatrix} \Sigma_A 1 & \Sigma_A \xi_A & \Sigma_A \eta_A \\ & \Sigma_A \xi_A \xi_A & \Sigma_A \xi_A \eta_A \\ \text{sym.} & & \Sigma_A \eta_A \eta_A \end{bmatrix}, \quad \mathbf{Q} = \begin{bmatrix} 1 & 1 & 1 & 1 \\ \xi_1 & \xi_2 & \xi_3 & \xi_4 \\ \eta_1 & \eta_2 & \eta_3 & \eta_4 \end{bmatrix}.$$

The stresses at integration points on ω_e are now easily found from (3.29). That is,

$$\mathbf{T}_{ij}^{\omega} = \mathbf{E} \mathbf{P}^{-1} \mathbf{Q} \mathbf{T}_{ij}^{\Omega}. \quad (3.30)$$

3.7 DISCRETE FORM OF THE NORMAL STRESS EQUATION

We return now to (3.27) and substitute for h and g . We also require the expression (2.18) for the normal to the surface. On a typical element ω_e we have, after transforming to the master element $\hat{\omega}$,

$$\begin{aligned}
 & \frac{Re^2}{S} \int_{\hat{\omega}} \left[\sum_{A=1}^3 g_A^{(e)} \hat{\psi}_A(\xi) \right] r(h) J \, d\xi \\
 & + \int_{\hat{\omega}} \left[\sum_{A=1}^3 g_A^{(e)} \hat{\psi}'_A(\xi) \right] \frac{h}{\sqrt{1+h^2}} \, d\xi \\
 & - a \int_{\hat{\omega}} \left[\frac{\sum_{A=1}^3 g_A^{(e)} \hat{\psi}_A(\xi)}{f \sqrt{1+h^2}} \right] J \, d\xi + \frac{h_0^{(1)} g_0^{(1)}}{\sqrt{1+h_0^{(1)2}}} \\
 & \equiv \mathbf{g}^{(e)T} \mathbf{F}^{(e)}(\mathbf{h}^{(e)}) \tag{3.31}
 \end{aligned}$$

where the last term on the left hand side applies only to the element ω_1 , $\mathbf{g}^{(e)}$ is the 3×1 vector of nodal values of g on ω_e , and $\mathbf{F}^{(e)}$ is a nonlinear function on $\mathbf{h}^{(e)}$. The function $r(h)$ arises from the

normal stress and is given by

$$\begin{aligned} r(\mathbf{h}) &\equiv \mathbf{T}\mathbf{n} \cdot \mathbf{n} = T_{ij}n_i n_j \\ &= \frac{T_{11}h^2 - 2T_{12}h + T_{22}}{(1 + h^2)} \end{aligned} \quad (3.32)$$

For convenience h has not been shown explicitly as a function of h_A on the left hand side of (3.31).

We introduce the global vectors \mathbf{g} and \mathbf{h} of nodal values of g and h on the free surface so that, using (3.27) and (3.31), the normal stress equation becomes

$$\mathbf{g}^T \mathbf{F}(\mathbf{h}) = 0$$

or, since \mathbf{g} is arbitrary,

$$\mathbf{F}(\mathbf{h}) = 0 \quad (3.33)$$

Equation (3.33) is a set of simultaneous nonlinear equations in \mathbf{h} , after the integrations in (3.31) have been carried out (note that in evaluating the first integral on the left hand side of (3.31), the expression (3.32) is used and the stress components are obtained at the integration points from (3.29)). Equation (3.33) is solved approximately by the Newton-Raphson method, that is, by the iterative process

$$\mathbf{h}^{(n+1)} = \mathbf{h}^{(n)} - (\mathbf{DF}^{(n)})^{-1} \mathbf{F}(\mathbf{h}^{(n)})$$

where DF is the tangent matrix associated with F :

$$(DF)_{ij} = \frac{\partial F_i}{\partial h_j} .$$

This is readily obtained at element level; for example, the contribution of the first term on the lhs of (3.31) to the tangent matrix is

$$\frac{Re^2}{S} \int_{\hat{\Omega}} \hat{\psi}_A(\xi) J(\xi) \left[\frac{dr}{dh} \right]^{(n)} \hat{\psi}_B(\xi) d\xi .$$

The other element contributions are obtained in a similar way, resulting in the element tangent matrix $DF^{(e)}$. The global tangent matrix is then obtained by the usual assembly process.

CHAPTER 4

SOLUTION ALGORITHM AND NUMERICAL RESULTS

4.1 SOLUTION ALGORITHM

The following overall algorithm is used to solve the equations (3.12–3.13) and (3.33). The problem is initialised by choosing the downstream length $L^{(0)}$. Also, an initial shape of $f^{(0)}$ of the free surface is assumed.

Generally, given $L^{(I)}$ and $f^{(i)}$ the auxiliary problem (3.12) – (3.13) is solved for $u^{(i+1)}$ and $p^{(i+1)}$, and the stress on the free surface is determined. Here the iteration counter (I) is temporarily suppressed for convenience.

The normal stress equation (3.33) is then solved for $h^{(i+1)}$ using the standard Newton–Raphson method, and this function is integrated to obtain $f^{(i+1)}$. If $\max|f^{(i+1)} - f^{(i)}| < \nu$ where ν is a prescribed tolerance, the solution $(u^{(I)}, p^{(I)}, f^{(I)})$ corresponding to a downstream length $L^{(I)}$ will have been obtained.

The downstream length L is now modified and the problem solved for the length $L^{(I+1)}$. This iteration terminates when the user is satisfied that L is long enough to have fully developed parallel flow downstream, at $x_1 = L$.

This overall algorithm is summarised in Figure 4.1.

Both the auxiliary problem and the normal stress equation are nonlinear, and these too have to be solved iteratively. In the case of the auxiliary problem it has been found by a number of authors (e.g. Engelman, Strang and Bathe (1981)) that the classical Newton-Raphson method does not perform well when applied to the Navier-Stokes equations. The problem that arises is that the radius of convergence is small; this means that a good starting value is needed for the procedure to converge to the required solution.

We shall discuss the method known as Picard iteration (also called successive substitution), which is used in the solution of the auxiliary problem. This method has a larger radius of convergence than the Newton method but its rate of convergence is relatively slow. The convergence rate of the Picard method is approximately linear while that of the Newton method is quadratic. The algorithm corresponding to solution of the auxiliary problem by Picard iteration is shown in Figure 4.2.

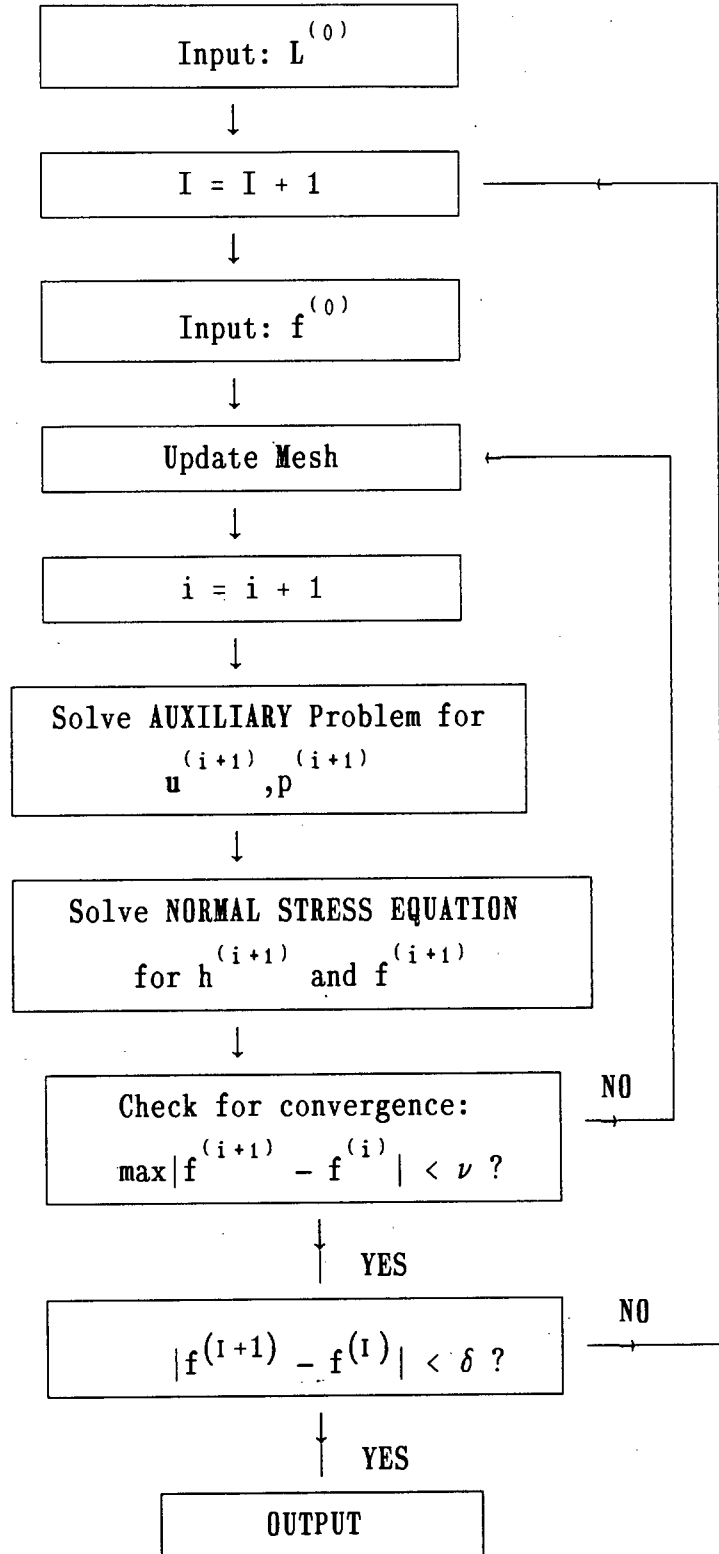


Figure 4.1 : The overall algorithm

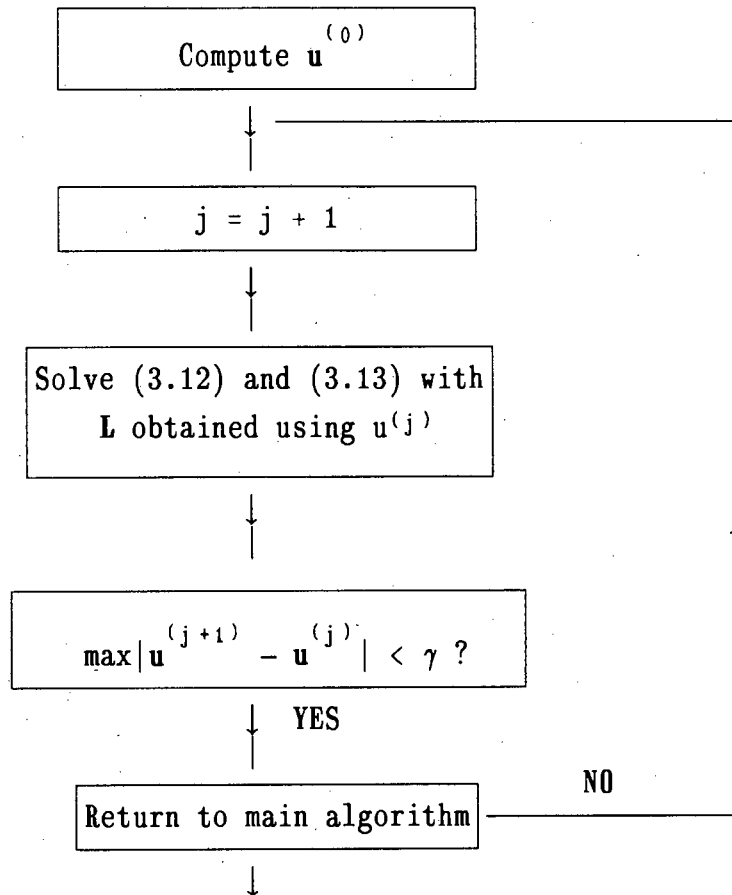


Figure 4.2 : Algorithm for solution of auxiliary problem

The algorithm summarised in Figure 4.2 converges for small Reynolds numbers, with $u^{(0)}$ obtained as the Stokes (linear) solution. However, as the Reynolds number increases the nonlinear convective term in the Navier-Stokes equation becomes dominant. This affects the numerical stability of the Gaussian elimination procedure (without pivoting) used to solve the system of equations derived from the Navier-Stokes equations. To overcome this difficulty, for large Reynolds numbers we use a method known as the continuation method, to obtain $u^{(0)}$. The idea behind this method is to generate a starting value which is in the radius of convergence.

To do this, we start with a small Reynolds number $Re^{(0)}$ ($= 1$, say) and solve the auxiliary problem. *This* solution is used as an initial guess $u^{(0)}$ corresponding to the solution of the problem at a Reynolds number $Re^{(1)} > Re^{(0)}$. This process continues until the desired Reynolds number is reached.

In the case of the normal stress equation we have seen in (3.27) that an estimate of f is required for the axisymmetric case, in order to solve for h . The values of f obtained in the previous iteration were used for this purpose.

4.2 NUMERICAL RESULTS

Computational aspects of this thesis have focused exclusively on the die-swell problem, illustrated in Figure 4.3. Note that the lengths shown are all dimensionless quantities, as discussed in Chapter 2.

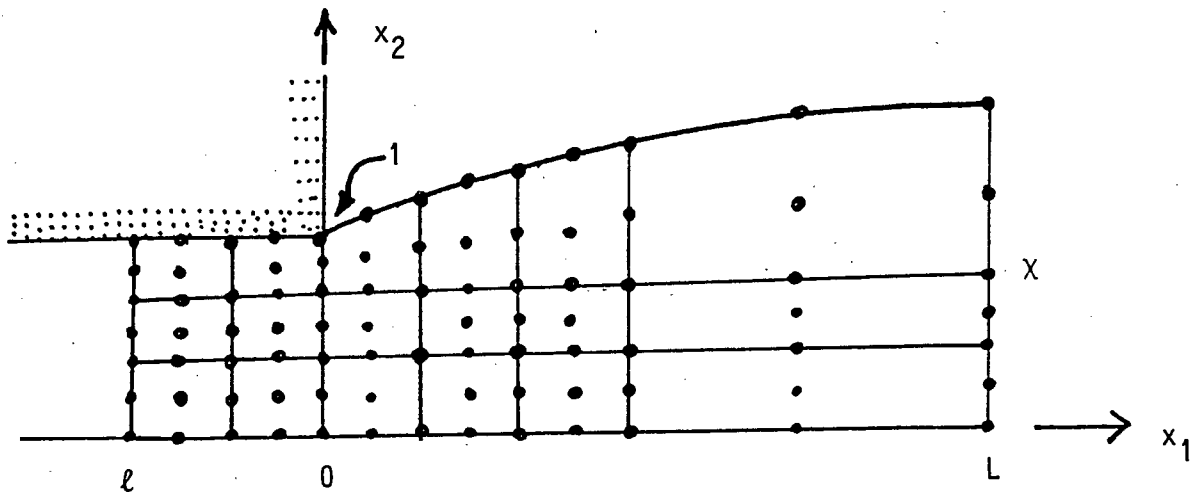


Figure 4.3 : The die-swell problem, with typical finite element mesh

The problem is characterised by the following features:

- (a) gravitational effects are neglected;
- (b) the flow is symmetric with respect to the x_1 -axis;
- (c) fully-developed Poiseuille flow exists at a distance ℓ upstream of the exit plane;
- (d) there is a uniform velocity field at a distance L downstream of the exit plane;
- (e) there is no zero pressure in the inviscid surrounding fluid.

We have implemented the algorithm described in Section 4.1 in a computer code. This code was written in FORTRAN and developments were carried out on a VAX 6320 computer at the University of Cape Town. A large amount of literature exists on the programming of the finite element method; we used as references the texts by Hinton and Owen (1979), Dhatt and Touzot (1984), Burnett (1982) and Hughes (1987).

The die-swell problem was solved numerically for Reynolds numbers in the range $1 \leq Re \leq 300$ and dimensionless surface tension coefficients in the range $0 \leq S \leq 150$.

The domain Ω is partitioned into quadrilaterals as shown in Figure 4.3. As stated earlier, we used $Q_2 - P_1$ element pair, that is, 9-noded quadrilaterals with biquadratic polynomials for the velocity and dimensionless linear polynomials for the pressure. It is worth

noting that Omodei (1979) partitioned his domain into quadrilaterals and each quadrilateral was then partitioned into four 15-degree of freedom triangles.

Various meshes were tried, and a mesh of the form shown in Figure 4.3 was eventually used for all problems since it gave sufficiently accurate results. The key feature of this mesh is the refinement in the region of the outlet. The downstream length required to capture fully-developed parallel flow was found to lie in the range $3.5 \leq L \leq 20$ while the upstream length ℓ was set at $\ell = -3.5$.

Gauss integration was used to evaluate all integrals: 2*2 integration was used to determine integrals over Ω_e or $\hat{\Omega}$ while 3-point integration was used for integrals over ω_e or $\hat{\omega}$. Numerical experiments were also run to determine the optimal tolerances ν , δ and γ appearing in the algorithms summarised in Figures 4.1 and 4.2. A value of $\nu = \delta = \gamma = 10^{-3}$ was found to be satisfactory. The penalty parameter ϵ in (3.13) was set at $\epsilon = 10^{-5}$, which was found to be satisfactory.

Table 4.1 gives details of the die-swell ratio χ (see Figure 4.3) for the *plane* problem, and for a range of values of Re and S . Also shown in the table are corresponding results obtained by Omodei (1979), where these are available. The various numbers of iterations required to achieve satisfactory results are also shown; these are all seen to be small, except at higher values of Reynolds numbers.

As can be seen in Table 4.1, there is generally good agreement between the results obtained here, and those obtained by Omodei (1979). The particular feature of these results is that swelling occurs for lower values of Re , but for values of Re exceeding 10, shrinkage occurs ($\chi < 1$). This phenomenon appears to be independent of the surface tension coefficient.

Surface profiles corresponding to the results in Table 4.1 are shown in Figures 4.4 and 4.5. Figure 4.4 gives a range of profiles for zero surface tension, while Figure 4.5 allows one to compare profiles for a particular value of Re and different values of S . Also shown in these figures are the profiles obtained by Omodei (1979).

Table 4.2 gives results along the lines of those displayed in Table 4.1, but for the *axisymmetric* problem. These results are compared with results obtained by Omodei (1980). There is very little qualitative difference between the results in the two tables; in particular, the phenomenon of χ decreasing with an increase in Re is again observed. Figures 4.6 and 4.7 show surface profiles corresponding to some of the results in Table 4.2, together with corresponding profiles obtained by Omodei (1980).

In all cases the algorithms described in Section 4.1 were found to be stable, in that convergence to within the specified tolerances occurred after relatively few iterations.

Table 4.1 : Results for the plane die-swell problem

Reynolds number (Re)	Surface tension parameter (S)	Present method				χ	χ Omodei (1979)
		Picard iterations	Continuation Method	Normal Stress Equation iterations	Free Surface Shape iterations		
1	0	2	1	1	2	1.200	1.191
	0.8					1.115	1.114
	1.5					1.029	-
4	0	2	1	1	2	1.148	1.166
	0.8					1.124	1.155
	1.5					1.110	-
10	0	2	1	1	2	1.075	1.078
25	0	3	2	1	2	0.977	0.959
	60					0.980	0.985
75	0	7	4	1	2	0.909	0.878
	150					0.877	0.895
300	0	9	5	1	2	0.845	0.844

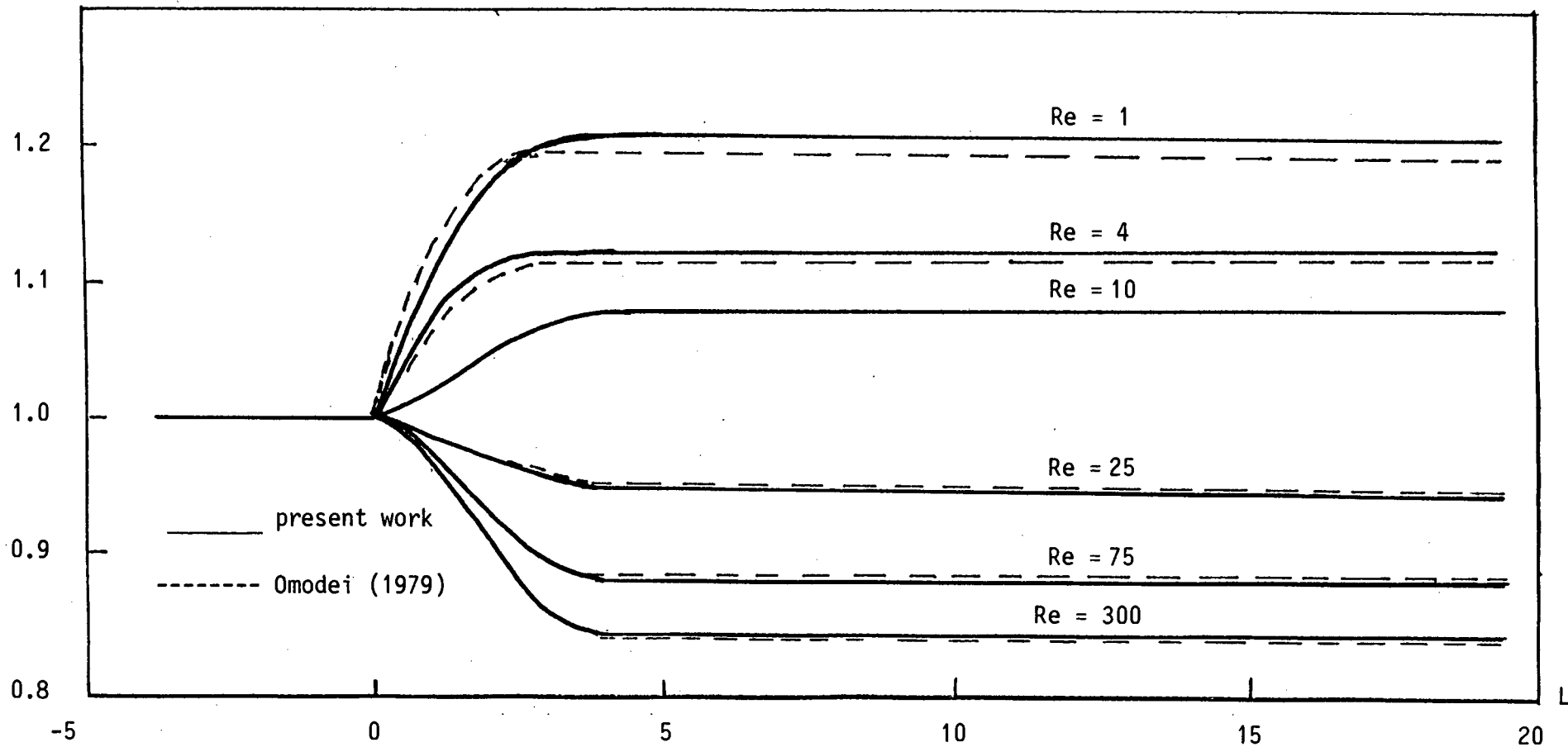


Figure 4.4 : Free surface profiles for the plane die-swell problem with zero surface tension

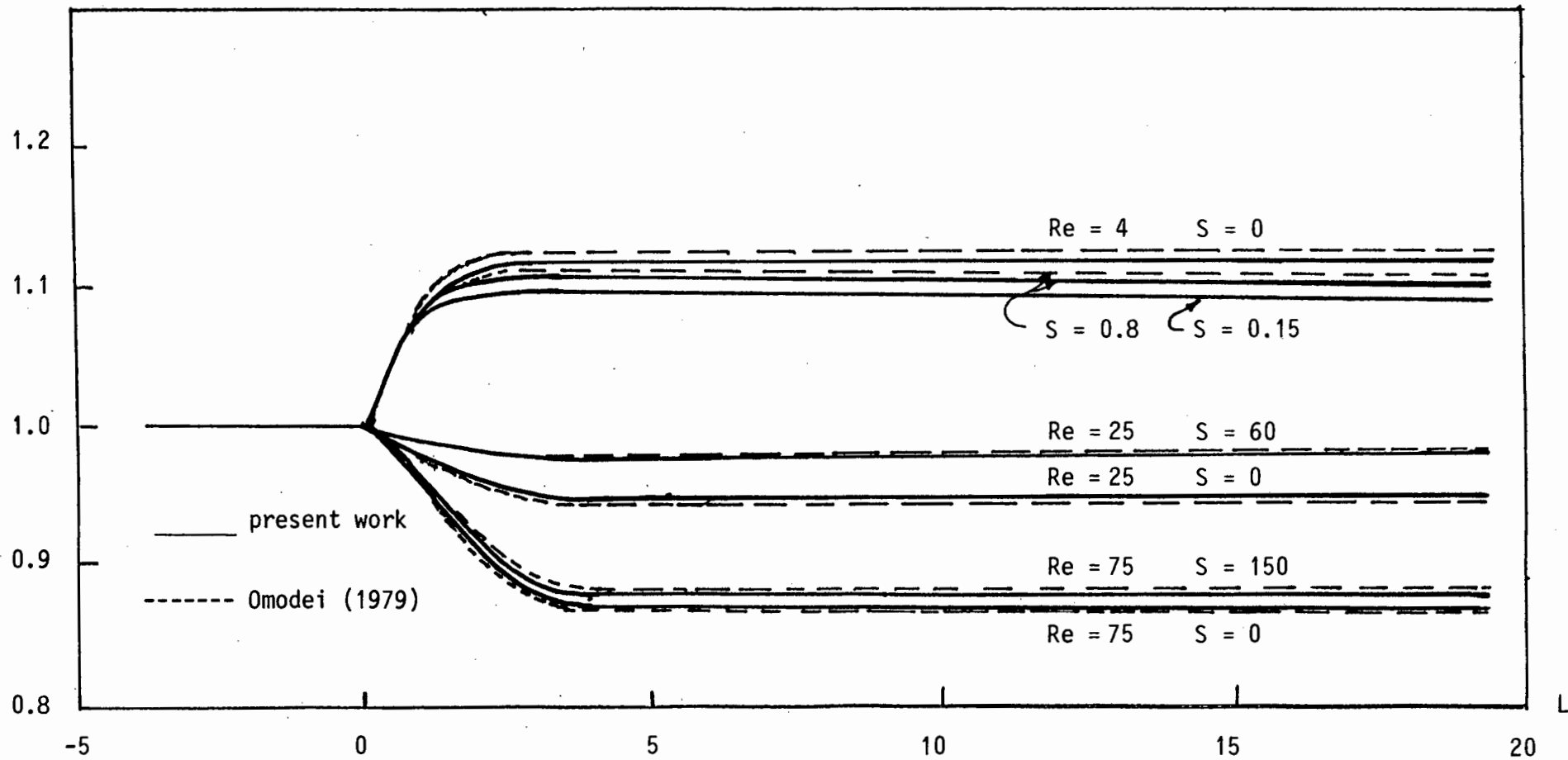


Figure 4.5 : Free surface profiles for $Re = 4, 25$ and 75 for the plane die-swell problem with various values of surface tension

Table 4.2 : Results for the axisymmetric die-swell problem

Reynolds number (Re)	Surface tension parameter (S)	Present method				χ	χ Omodei (1980)
		Picard iterations	Continuation Method iterations	Normal Stress Equation iterations	Free Surface Shape iterations		
1	0	2	1	1	1	1.220	—
4.2	0	3	3	1	1	1.120	1.102
	1.2					1.090	1.088
	2.4					1.075	1.077
10	0	3	3	1	1	1.030	—
24	0	3	2	1	1	0.956	0.954
65	0	7	5	1	1	0.908	0.901
300	0	9	5	1	2	0.888	—

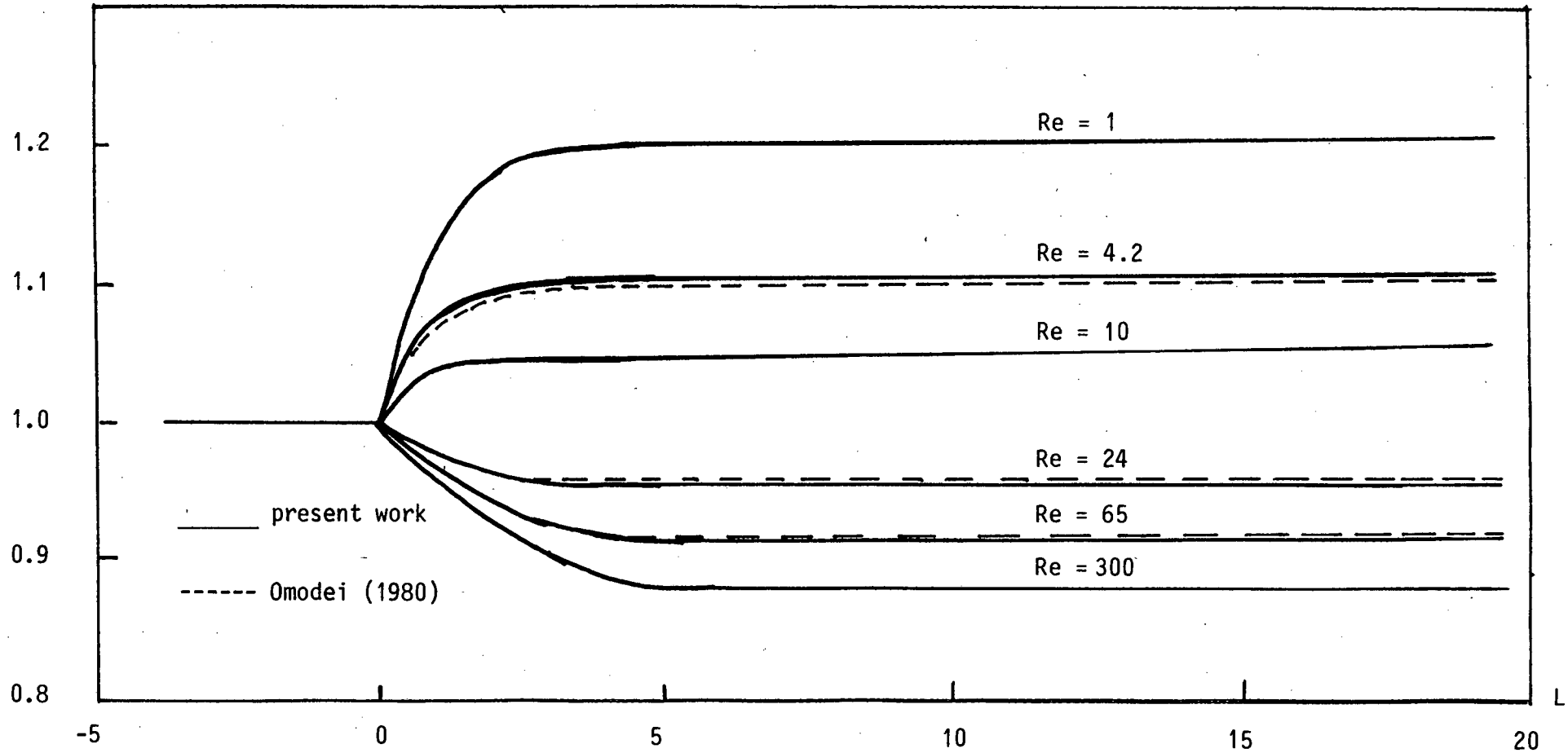


Figure 4.6 : Free surface profiles for the axisymmetric die-swell problem with zero surface tension

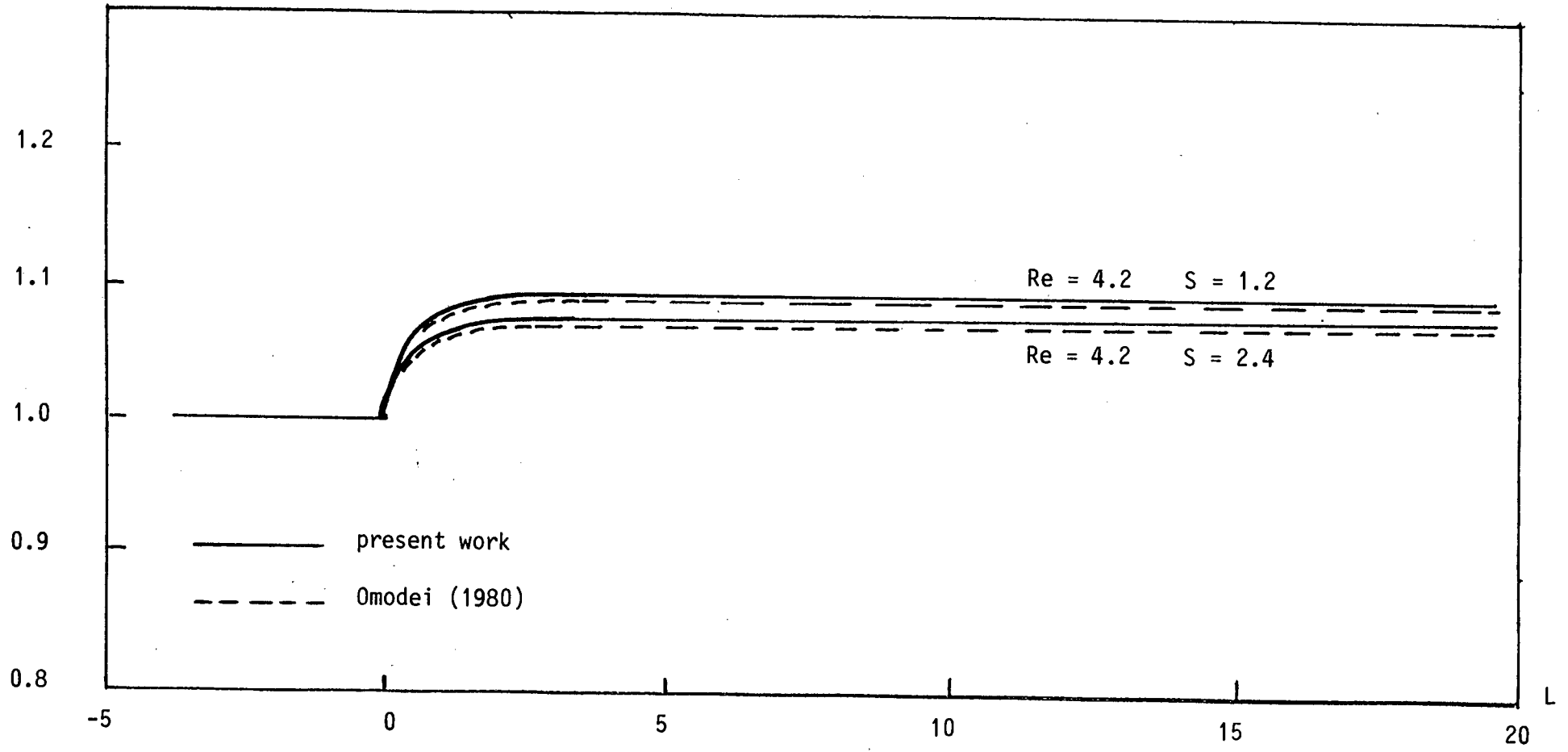


Figure 4.7 : Free surface profiles for the axisymmetric die-swell problem with $S = 1.2$ and 2.4

CHAPTER 5

DISCUSSION AND CONCLUSIONS

We have studied plane and axisymmetric free surface problems for viscous flows. The general problem is subdivided into two parts: the auxiliary problem, in which the Navier-Stokes equations are solved assuming the free surface to be fixed; and the normal stress equation, which is used to solve for the shape of the free surface. This subdivision has formed the basis of the predictor-corrector algorithm.

Both the auxiliary problem and the normal stress equation have been put into variational form, and finite element approximations have been developed. For the auxiliary problem the velocity and pressure have been approximated by nine-noded biquadratic elements and discontinuous linear pressures respectively, a combination which is known to be unconditionally stable. The unknown function in the normal stress equation is the slope to the free surface, which is approximated by one-dimensional piecewise quadratic functions.

The method developed here has been applied to the die-swell problem. Various iterative procedures have been used to solve the pair of equations. These include Picard iteration for the nonlinear convective term, a continuation method for obtaining solutions at high Reynolds numbers, a standard Newton-Raphson method for the solution of

the normal stress equation, and finally an overall iterative process for correcting the shape of the free surface. The algorithms described in Chapter 4 have all performed well for the range of parameters studied, in the sense that convergence to acceptable solutions was reached with relatively few iterations. Furthermore, results generally compare well with computational results obtained by Omodei (1979,1980). We have been able to obtain results of acceptable accuracy using a relatively coarse mesh compared to that used by Omodei.

Various extensions of the present work are evident, and also desirable. First, an important extension would be to the case of non-steady flows; it would be interesting to investigate the performance of the procedure discussed here, to that case. Also, it is of interest to investigate a wider range of problems, and to extend the formulation to the case of genuinely three-dimensional flows. In the latter case computer speed and memory will be important considerations.

REFERENCES

ASAITHAMBI, N S (1987)

Computation of free surface flows. *Jour. Comp. Phys.* **73**,
380-394.

BURNETT, D S (1987)

Finite Element Analysis, From Concepts to Applications. Addison
Wesley, New York.

CAREY, G F and ODEN, J T (1982)

Finite Elements: A Second Course. Prentice-Hall, New Jersey.

CHAN, S T K and LAROCK, B E (1973)

Fluid flows from axisymmetric orifices and valves. *Jour. Hydr.*
Div. proc. ASCE, **99**, 81-87.

CHAN, R K C and CHAN, F W K (1980)

Numerical solution of transient and steady free-surface flows
about a ship of general hull shape. *13th Symp. Naval Hydrodyn.*
Tokyo, Japan, 257-280.

CUVELIER, C and SCHULKES, R M S M (1990)

Some numerical methods for the computation of capillary boundaries governed by the Navier-Stokes equations. *SIAM Review*, **32**, 3, 355-423.

DHATT, G and TOUZOT, G (1984)

The Finite Element Method Displayed. Wiley, New York.

DYM, C L (1974)

Introduction to the Theory of Shells. Pergamon Press, Oxford.

ENGELMAN, M S, STRANG, G and BATHE, K J (1981)

The application of quasi-Newton methods in fluid mechanics. *Int. J. Numer. Meth. Engng.* **17**, 709-718.

GEORGIU, C G, SCHULTZ, W W and OLSON, L G (1990)

Singular finite elements for the sudden-expansion and the die-swell problems. *Int. Jour. Numer. Meth. Fluids*, **10**, 357-372.

HAUSSLING, H J and COLEMAN, R M (1979)

Nonlinear water waves generated by an accelerated circular cylinder. *Jour. Fluid Mech.* **92**, 767-781.

HINTON, E and OWEN, D R J (1977)

Finite Element Programming. Academic Press, London.

HO, Lee-Wing and PATERA, Anthony T (1990)

A Legendre spectral element method for simulation of unsteady incompressible viscous free surface flows. *Comp. Meth. Appl. Engng.* 80, 355-366.

HO, Lee-Wing and PATERA, Anthony T (to appear)

Variational formulation of three-dimensional viscous free surface flows. *Int. Jour. Numer. Meth. Fluids.*

HUGHES, Thomas J R (1987)

The Finite Element Method, Prentice-Hall, New Jersey.

JEAN, M and PRITCHARD, W G (1980)

The flow of fluids from nozzles at small Reynolds numbers. *Proc. R. Soc. Lond.* A370, 61-72.

JOSEPH, D D (1976)

Stability of Fluid Motions: Volume 2, Springer, Berlin.

KRUYT N P, CUVELIER, C, SEGAL, A and VAN DER ZANDEN, J (1988)

A total linearization method (TLM) for solving viscous free boundary flow problems by the finite element method. *Int. Jour. Numer. Meth. Fluids*, 8, 351-363.

LAROCK, B E and TAYLOR, C (1976)

Computing three-dimensional free surface flows. *Int. J. Meth. Engng.* 10, 1143-1152.

LE ROUX, C and REDDY, B D (to appear)

Mixed Variational Problems Associated with Viscous Incompressible Free-Boundary Flows. *Nonl. Anal.: Theory, Meths. and Appls.*

NICKELL, R E, TANNER, R I and CASWELL, B (1974)

The solution of viscous incompressible jet and free surface flows using finite element methods. *Jour. Fluid Mech.* **65**, 189-206.

OMODEI, B J (1979)

Computer solutions of a plane Newtonian jet with surface tension. *Comp. Fluids*, **7**, 79-96.

OMODEI, B J (1980)

On the die-swell of an axisymmetric Newtonian jet. *Comp. Fluids*, **8**, 275-289.

PUKHNACHOV, V (1972)

A plane steady-state free boundary problem for the Navier-Stokes equations. *Appl. Mech. Tech. Phys.* **3**, 91-102.

REDDY, B D (1986).

Functional Analysis and Boundary Value Problems: An Introductory Treatment. Longman, London.

RUSCHAK, K J and SCRIVEN, L E (1977).

Developing flow on a vertical wall. *Jour. Fluid Mech.* **81**, 305.

TANNER, R I, NICKELL, R E and BILGER, R W (1975).

Finite element methods for the solution of some incompressible non-Newtonian fluid mechanics problems with free surfaces.

Comp. Meth. Appl. Mech. Engng., **6**, 155-174.

THOMPSON, E G, MARK, L R and LIN, F S (1969).

Finite element method for incompressible slow viscous flow with a free surface. *Dev. in Mech.*, **5**, 93.

WILLIAMSON, A S (1972).

The bearing of an adhesive layer between flexible tapes pulled apart. *Jour. Fluid Mech.*, **52**, 639-656.